Theme VIa: Checking of actual structures

Objekttyp: **Group**

Zeitschrift: **IABSE congress report = Rapport du congrès AIPC = IVBH Kongressbericht**

Band (Jahr): **9 (1972)**

PDF erstellt am: **21.07.2024**

VI

Etudes expérimentales du comportement des ouvrages sous les sollicitations

Experimentelle Studien über das Verhalten der Bauwerke unter Belastung

Experimental Study of the Behaviour of Structures under Loads

VI a

Contrôle des ouvrages existants

Kontrolle bestehender Bauten

Checking of Actual Structures

Leere Seite

Blank page

Page vide

Kontrollmessungen an Brückenkonstruktionen

Control Measurements of Bridges

Mesures de contrôles de ponts

A. SZITTNER
TU Budapest, Lehrstuhl für Stahlkonstruktionen
Budapest, Ungarn

Die Mitarbeiter des Lehrstuhles für Stahlkonstruktionen der TU Budapest haben in den letzteren Zeiten an den in Ungarn gebauten verschiedenen Brückenkonstruktionen Kontrollmessungen durchgeführt, um die wirkliche und theoretische Kräftespiele gegenüberzustellen. Die Messungen wurden in fünf Gruppen klassiert:

1. Traditionelle Probebelastung,
2. Lastenzug-Einflusslinie,
3. Dynamisches Verhalten der Brücken,
4. Feststellung des Brückenzustandes,
5. Kontrollmessungen während des Baues.

Die Mess- und Auswertungsmethode bzw. die Folgerungen werden auf Grund der Messungen an den untenstehenden Strassenbrückenkonstruktionen vorgestellt:

a/ Hängebrücke mit Spannweite 44 + 290 + 44
b/ Verbundkonstruktion mit Kastenträger (Spannweite: 30 m)
c/ Durchlaufende Fachwerkbrücke mit Eisenbeton-Fahrplatte als Verbundkonstruktion mit Querträger (Spannweite: 3x70 m)
d/ Durchlaufende Verbundkonstruktion mit Kastenträger (Spannweite: 3x25 + 40 + 2x25 m)
e/ Durchlaufende Vollwand-Verbundkonstruktion mit Freikabel-Vorspannung (Spannweite: 57 + 67 + 57 m).

1. Traditionelle Probebelastung

Der Inbetriebnahme der Brücken geht immer ein amtlicher Prozess, die Probebelastung voran, wo den Vorschriften nach, nur die Durchbiegungen gemessen werden sollen. So wird das Kräftespiel und das Verhalten der Konstruktion im Ganzen kontrolliert. Im wissenschaftlichen und praktischen Sinne ist es aber auch wichtig, die wirklichen Spannungen und Beanspruchungen der Brückenelemente mit den theoretischen Werten, gewonnen an den mathematischen Modellen, zu vergleichen.

Durch die Messungen werden

die örtlichen Spannungen und Spannungsspitzen,
die Knotenpunkt-Nebenspannungen,
die Querverteilung und Torsionssteifigkeit, und
die Fahrbahn-Mitwirkung

kontrolliert.

Als Mess-System wurden bei den obenerwähnten Aufgaben Dehnungsmess-Streifen (DMS) mit Messverstärker und mit Registriereinrichtung, oder Dehnungsmesser mechanischen Systems angewendet.

Über die Messungen der örtlichen Spannungen kann nichts Neues gesagt werden. Um die Knotenpunkt-Nebenspannungen festzustellen, wurden die Spannungen (Dehnungen) neben den ausgewählten Knotenpunkten auf jedem Stab bei der Stabmitte und neben dem Knotenblech in den 4 Eckpunkten der Querschnitten gemessen. Auf Grund des Bernoulli-Navier-Satzes werden aus den Messergebnissen die Werte σ_N, σ_{Mx}, σ_{My} und σ_W gerechnet. Auf der Brückenkonstruktion nach Abb.4. in den Knotenpunkten 25 und 28 wurden die Nebenspannungen festgestellt. Bei den Gurtstäben sind die gemessenen Werte ein wenig höher als die gerechneten Werte nach Hartmann-Melan [1], aber bei den Diagonalen, wo die Stabkräfte bzw. die σ_N-Spannungen im absoluten Sinne kleiner sind, sind die Nebenspannungen prozentuell viel höher. Auf Abb.1. wurde die Tendenz vorgestellt, dass die Knotenpunkt-Nebenspannungen mit der Zunahme der Ausnützung des Stabes sich vermindern. Die Nebenspannungen waren immer beachtlich [2].
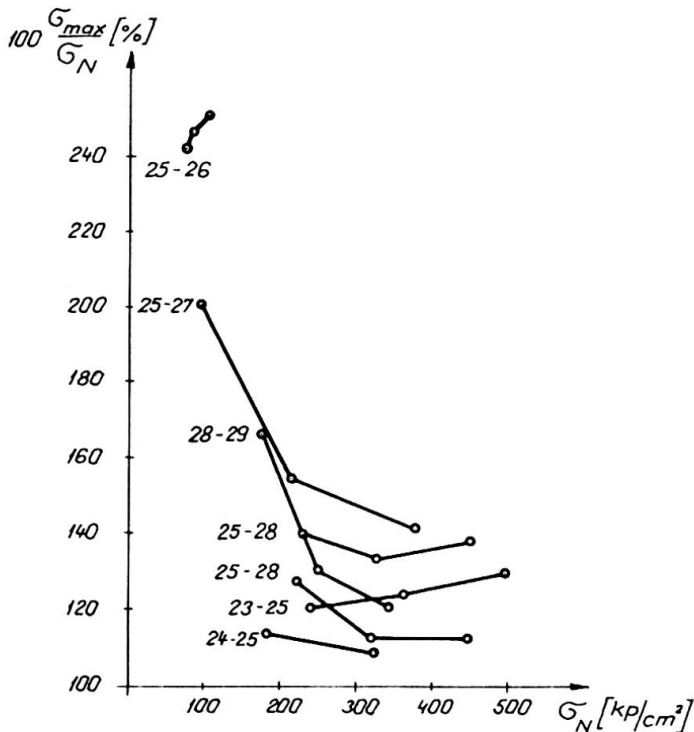

Abb.1.

Auf dieser Brücke wurde auch die Querverteilung kontrolliert. Die Messergebnisse und die Werte - gerechnet nach Cornelius [3] - zeigten weder bei symmetrischer, noch bei asymmetrischer Belastung gute Übereinstimmung. Die Messergebnisse unterstützten viel mehr eine Rechenmethode wobei die Konstruktion als einfacher Träger auf zwei Stützen gerechnet wurde (Abb.2.).

An der selben Konstruktion wurde auch die Mitwirkung der Fahrbahnkonstruktion überprüft. Die Spannungen in dem Untergurt sind wegen der Mitwirkung der Fahrbahnplatte etwa 20-30 % kleiner, als die ohne Mitwirkung gerechneten Werte. Dementsprechend sind aber die Obergurt-Kräfte durch die Verkürzung des Hebelarmes der Zug-Druckkraft etwa 10-15 % höher, als die Werte einfach berechnet.

Diese Differenz vermindert sich bedeutend neben den Stützen, wo
die Fahrbahnplatte untergebrochen ist.

2. Lastenzug-Einflusslinien

Im Laufe der traditionellen Probebelastung werden die bei
einer genau bestimmten Achsenanordnung gemessenen und berechneten
Deformationen und Spannungen verglichen. Man bekommt aber ein besseres Bild über das Verhalten der Konstruktion, oder Konstruktionselemente, wenn die Belastung mit der Hilfe eines in der Fahrbahnachse sich langsam bewegenden Schwerlastwagens wirkt, und die Spannungen und Deformationen mit einer Registriereinrichtung aufgenommen werden. Die auf Grund der Einflusslinien gerechneten Werte werden den wirklichen Registratumwerten gegenübergestellt.

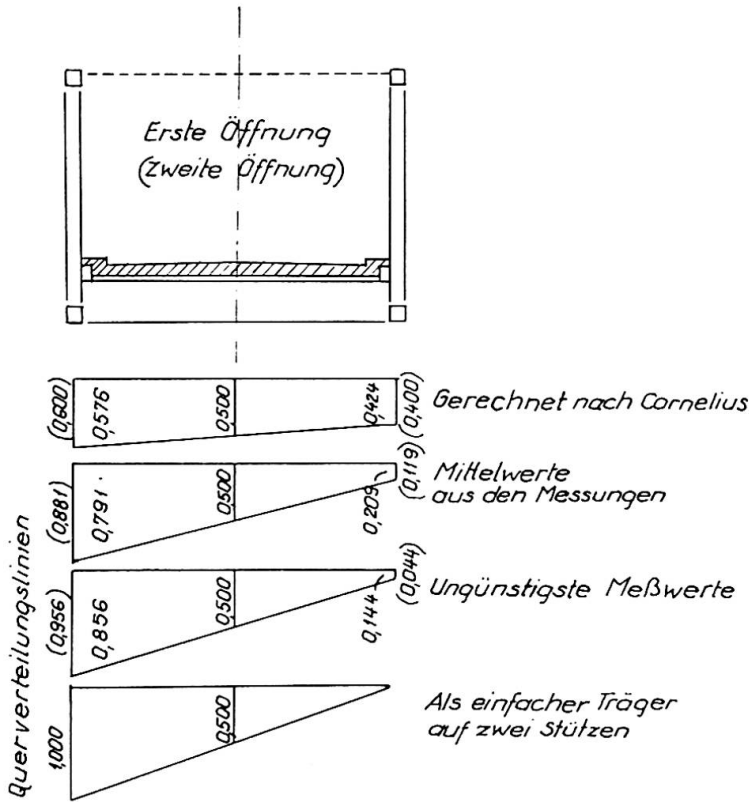Abb.3. zeigt die Gegenüberstellung der Lastenzug-Einflusslinie bei einer Verbund-Konstruktion mit Kastenträger (l = 30 m).
Die auf den verschiedenen Punkten des Kastenträgergurtes gemessenen Spannungen zeigen gut die Spannungsverteilung der Brücke. Der Durchschnittswert der Messergebnisse stimmt sehr gut mit dem gerechneten Wert [4].

Abb.2.

Abb.3.

Abb. 4.

Verbundkonstruktion
mit 3×6 Freikabel
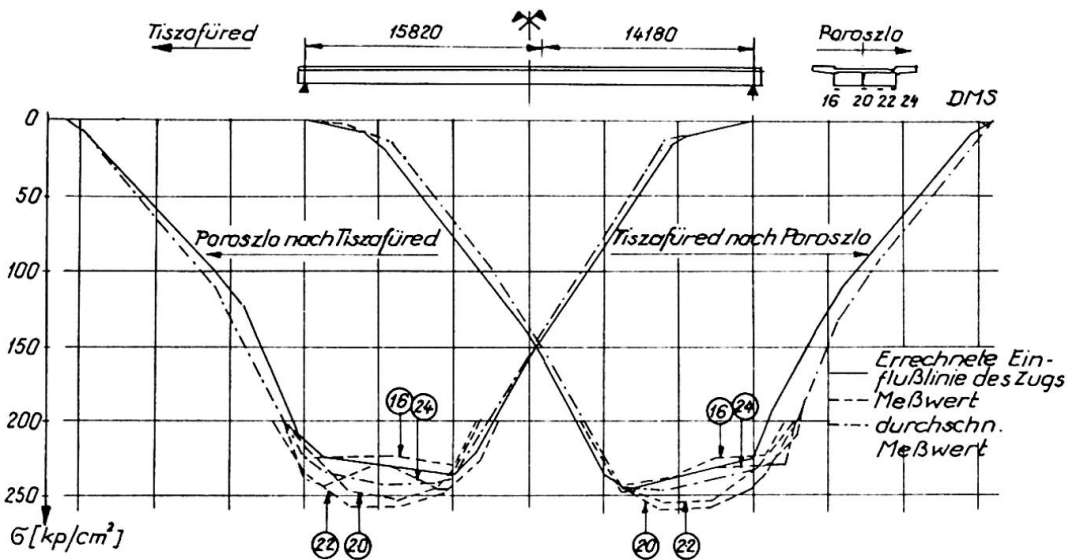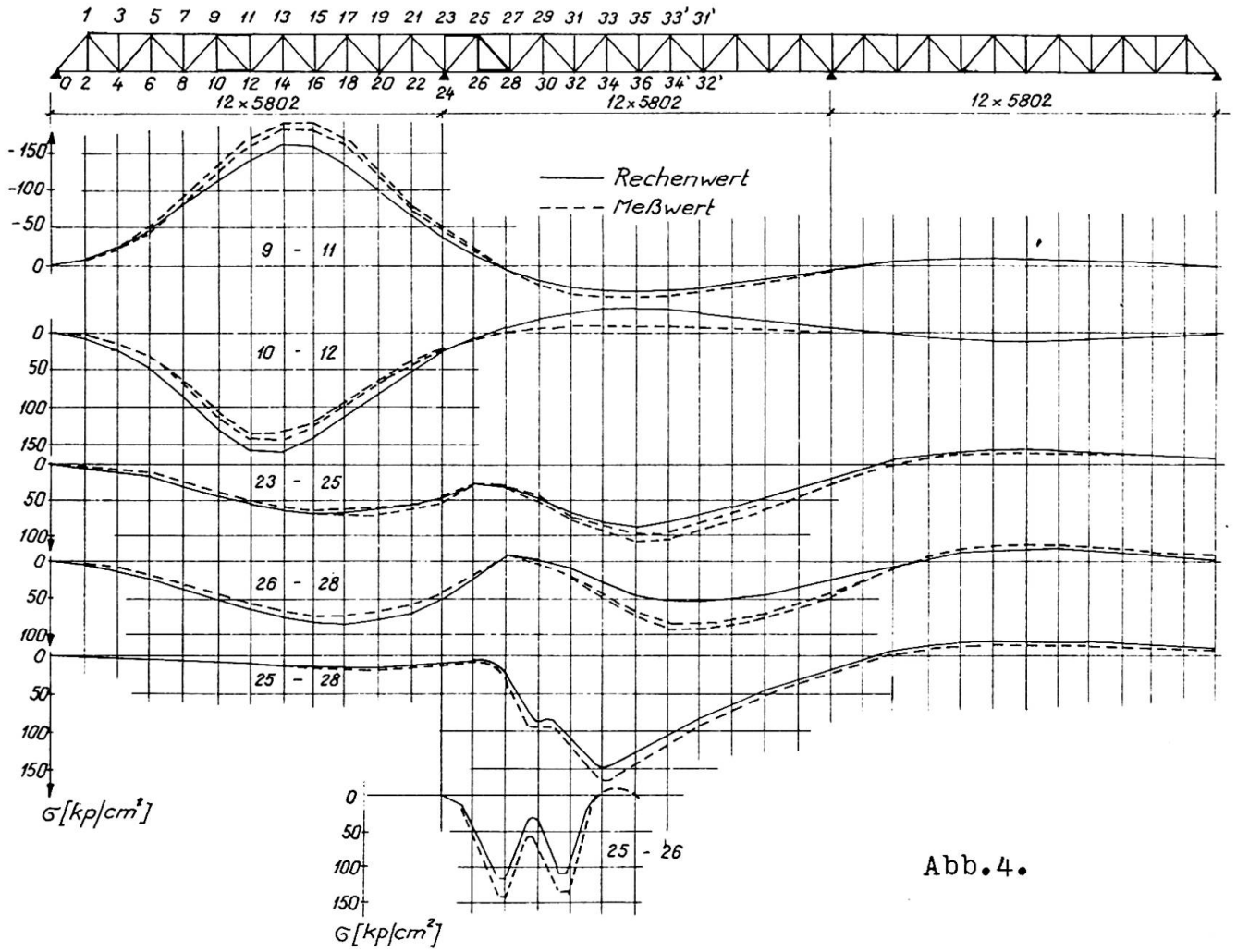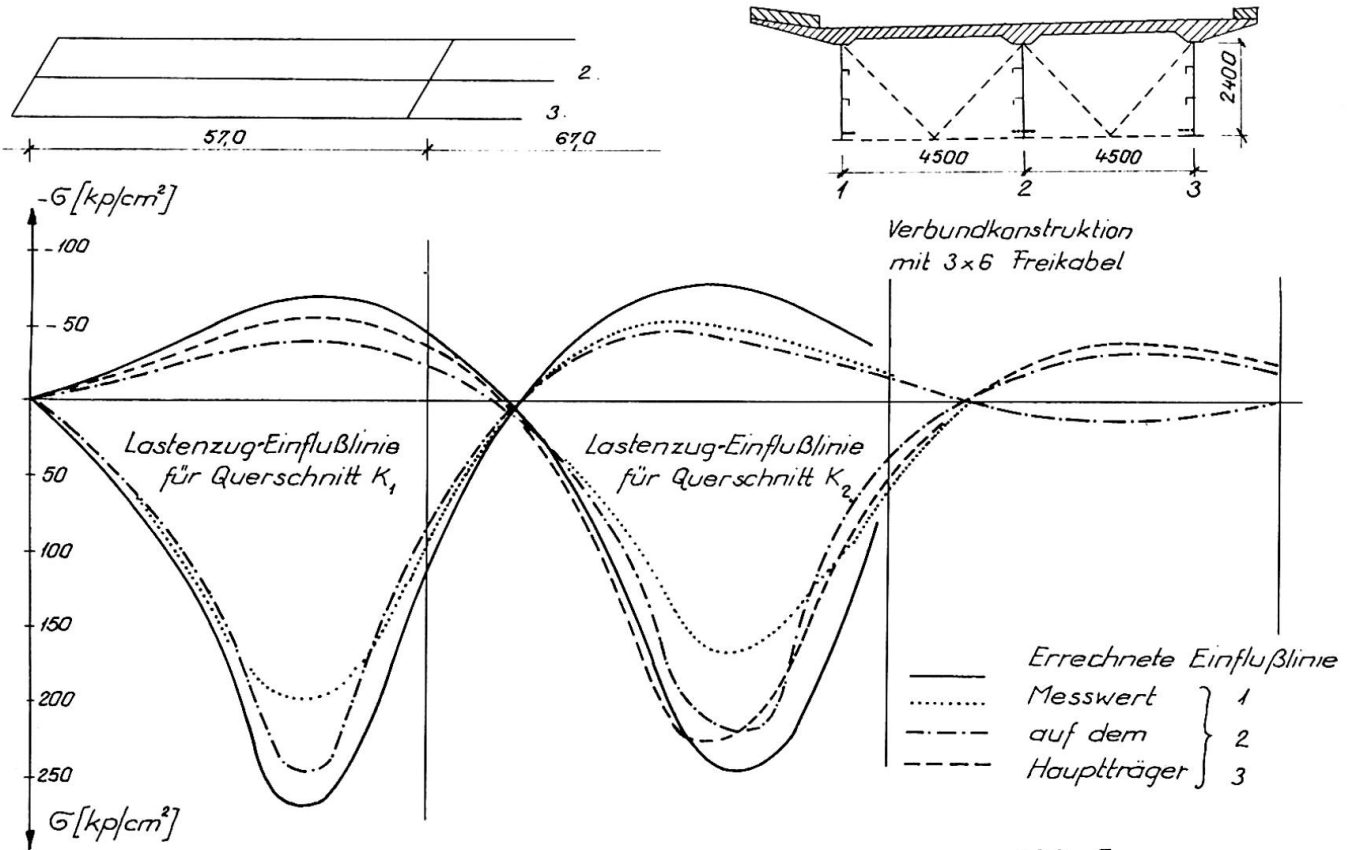
Abb. 5.

Auf Abb.4. sind die Lastenzug-Einflusslinien für die Stab-
spannungen eines durchlaufenden Fachwerkträgers zu sehen. Der
Ursprung der Abweichung zwischen den gerechneten und gemessenen
Spannungen ist auch jetzt die Mitwirkung der Fahrbahnplatte.
Deswegen ist die Obergurtkraft etwa 20 % höher, die Untergurt-
kraft etwa 10 % niedriger, als die ohne Mitwirkung der Fahrbahn-
platte gerechneten Werte. Bei dem Obergurt 23-25 gab es in der
Seitenöffnung infolge der Fahrbahnplatten-Unterbrechung keine
bedeutende Differenz, aber in der Mittelöffnung war die Diffe-
renz schon beachtlich.

In dem Gurtstab 26-28, wo die Stabkräfte etwas kleiner sind,
ist die Abweichung ein bischen grösser. Die Differenz meldet sich
besonders in dem Charakter der Einflusslinie. Bei den Diagonalen
25-28 und 25-26 ist die Abweichung nicht bedeutend.

Die Lastenzug-Einflusslinien geben ein sehr gutes Bild über
die Querverteilung der kastenartig ausgebildeten Brückenquer-
schnitten. Als Beispiel werden die Messergebnisse einer mit äus-
seren Kabeln gespannten, schrägen, durchlaufenden Verbundkonstruk-
tion erwähnt (Abb.5.). Wegen des schrägen Grundrisses und der
asymmetrischen Fahrbahn-Anordnung sind die Spannungen in den drei
Hauptträgern verschieden, andererseits wegen der besseren Beton-
qualität etwas kleiner, als die nach dem Entwurf gerechneten
Werte.

3. Dynamisches Verhalten der Brücken

Die meisten Bemessungsvorschriften berücksichtigen die aus
der Bewegung stammende dynamische Zusatzlast mit einem sogenann-
ten dynamischen Faktor, der von der Art der Brücken abhängt und
mit der Spannweite sich vermindert. Bei einer konkreten Konstruk-
tion ist die Zusatzlast proportional mit der Nutzlast. Diese Vor-
aussetzung wurde durch die experimentellen Werte nicht unterstützt.
Deshalb bestrebte man theoretisch oder experimentell einen Zusam-
menhang, der das dynamische Verhalten der Brücken treu spiegelt.
Die Grunderscheinungen und die Grundgleichungen der Lösung sind
theoretisch klar (Effekt von Timoshenko, Zimmermann, usw.), aber
eine allgültige Superpositionsregel oder ein Zusammenhang der dy-
namischen Wirkung ist wegen der zeitlichen und räumlichen Zufäl-
ligkeit der Lasten unmöglich zu finden.

Aus diesem Grunde hat der UIC-ORE (Internationaler Eisen-
bahnverband, Forschungs- und Versuchsamt) für Eisenbahnbrücken
eine umfangreiche Experiment-Serie angefangen und die Messergeb-
nisse ausgewertet. In der zusammenfassenden Veröffentlichung [5]
hat der ORE die eindeutige Folgerung festgestellt, dass es unmög-
lich ist, die wirkliche dynamische Wirkung in geschlossener Form
sogar bei zwangsbahnartiger
Eisenbahn-Belastung festzu-
stellen. Die Anwendung des
dynamischen Faktors als Be-
messungsmethode spiegelt das
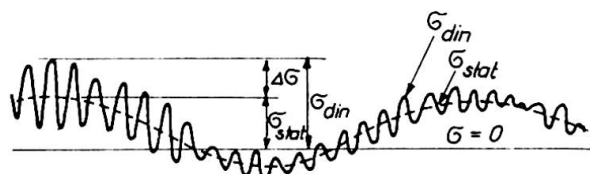wirkliche Kräftespiel nicht.

Abb.6.

Gleichzeitig mit den anderen Probebelastungen wurde in dem Geist der Arbeit von UIC-ORE auch dynamische Probebelastung durchgeführt, wo die Lastkraftwagen auf der Brücke in verschiedenen Gruppen und mit verschiedener Geschwindigkeit gefahren wurden.

Die Auswertung der Registraten wurde nach der Abb.6 gemacht. So wurden die charakteristischen Werte von σ_{stat}, σ_{din}, $\mu = \sigma_{din}/\sigma_{stat}$ und $\Delta\sigma = \sigma_{din} - \sigma_{stat}$ für jede Fahrt festgestellt. Mit verschiedenen Lastgruppen wurde erreicht, dass die Ausnützung der Träger verschieden sei. Als Ausnützung wurde ein prozentuelles Verhältnis zwischen dem Messwert σ_{stat} und dem Rechenwert $\sigma_{stat,max}$ genommen.

So wurden die Ergebnisse als Funktion der Ausnützung erstens auf Grund des dynamischen Faktors μ, zweitens auf Grund des dynamischen Mehrwertes $\Delta\sigma$ aufgezeichnet. Wenn die Hüllkurve dazu eingezeichnet wird, ist der Charakter des dynamischen Faktors, bzw. des dynamischen Mehrwertes sehr schön zu sehen.
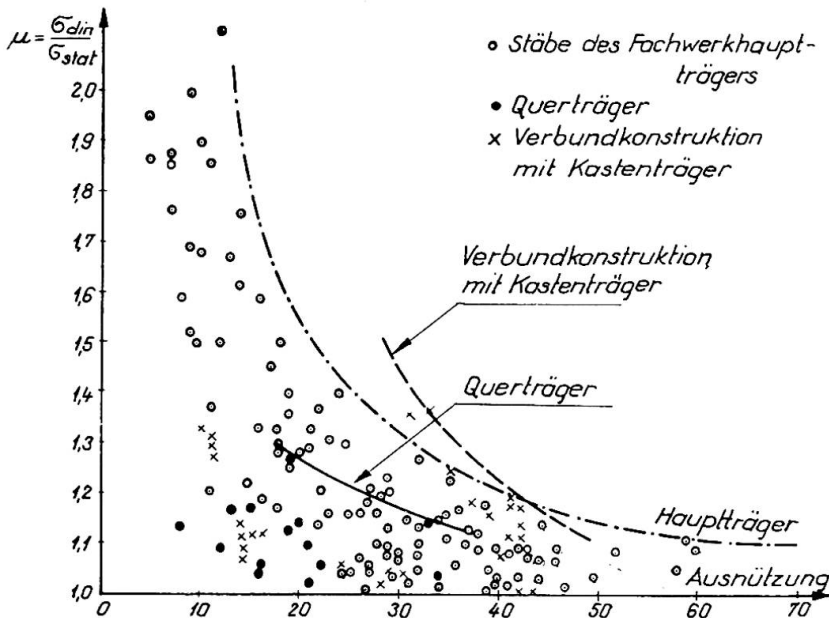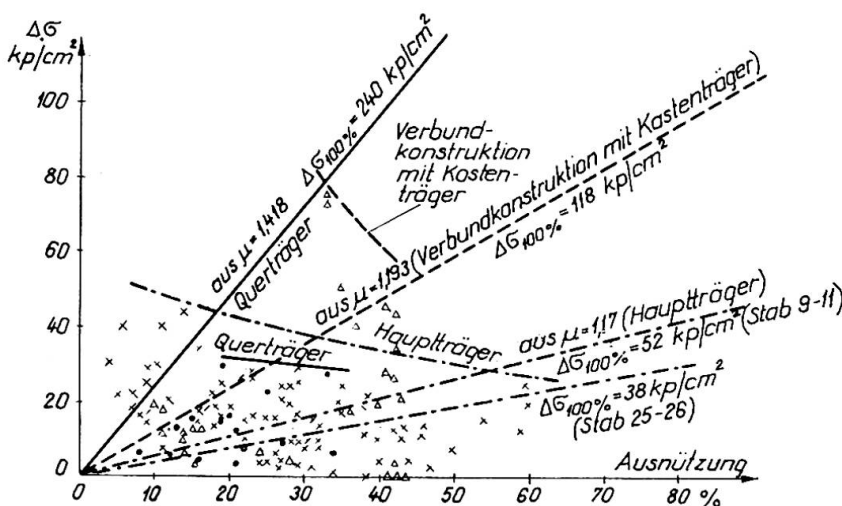

Abb.7.

Abb.8.

Als Beispiel wird auf den Abbildungen 7. und 8. die Auswer-
tung der Messergebnisse der Brücke von Tiszafüred (Fachwerkträger
und Vollwandträger siehe auf Abb.3,4); auf der Abb.9. die Auswer-
tung der Messergebnisse der Elisabeth-Brücke, und auf Abb.10. die
Auswertung der Messergebnisse einer durchlaufenden Verbundkon-
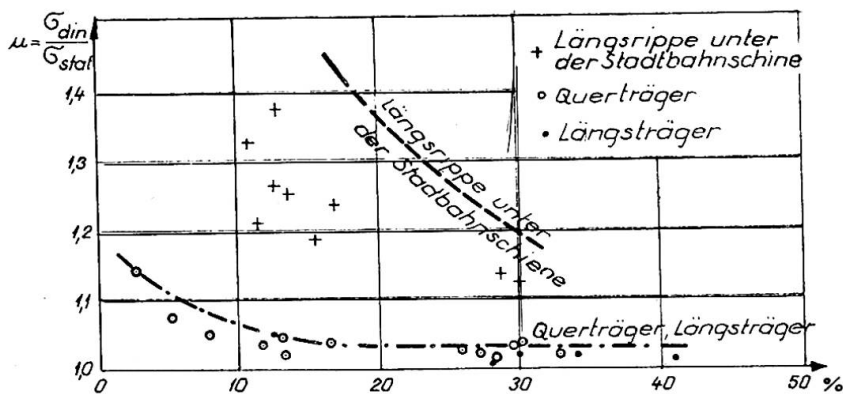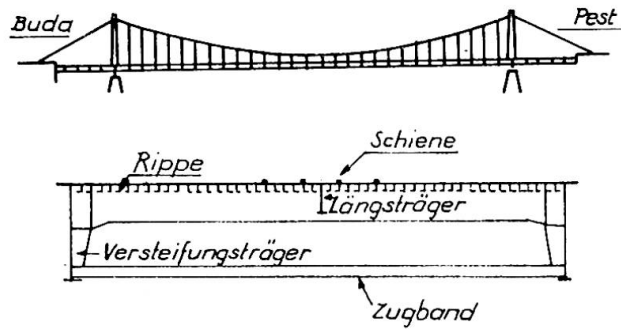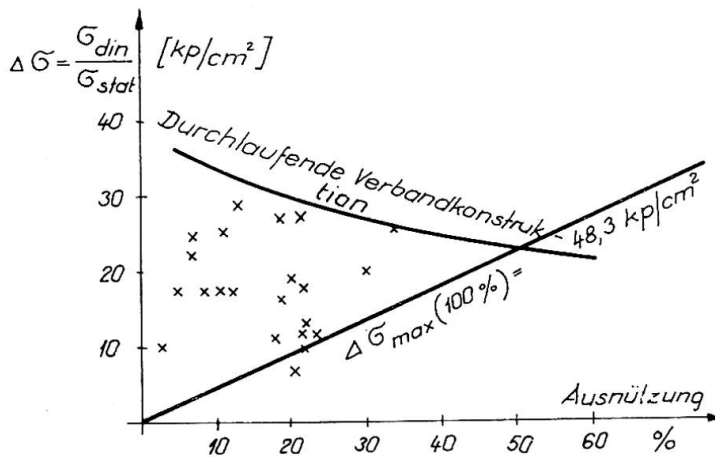struktion vorgestellt.

Abb.9.

Abb.10.

Auf Grund der Messergebnisse wurden die nachstehenden Folgerungen festgestellt:

a/ Der Wert von $\tilde{\sigma}_{din}/\tilde{\sigma}_{stat}$ ist kein Konstant, es vermindert sich mit dem Wachsen der Ausnützung.

b/ Der dynamische Mehrwert ($\tilde{\sigma}_{din} - \tilde{\sigma}_{stat}$) vermindert sich in Tendenz, oder stagniert.

c/ Die dynamische Vollbelastung der Strassenbrücken ist unmöglich. Unseren Erfahrungen nach ist die maximale Ausnützung etwa 60-70 %.

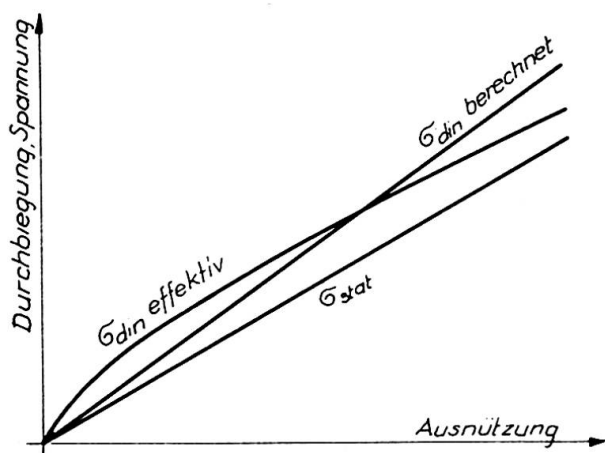d/ Bei der Dimensionierung der Strassenbrücken wäre auch richtiger, so wie es von UIC-ORE vorgeschlagen wurde, statt des dynamischen Faktors den dynamischen Mehrwert anzuwenden (Abb.11.).

Abb.11.

4. Feststellung des Brückenzustandes

Bei den neueren Brückenkonstruktionen, besonders bei den Stahlbeton- und Verbundkonstruktionen, wurden auf Grund des Vorschlages von I. Illésy die Eigenfrequenzen der Konstruktion auch gemessen. Es ist nämlich selbstverständlich, dass die nicht gut sichtbaren mechanischen Aenderungen (Risse, Stützenbewegungen usw.) auch die gut messbare Eigenfrequenz verändern können. Die Eigenfrequenzmessungen sind auf den neueren Brücken durchgeführt und ständig kontrolliert worden. Über die Erfahrungen kann noch nicht berichtet werden.

5. Kontrollmessungen während des Baues

Im Laufe der Bauzeit ist es sehr wichtig, besonders bei den durchlaufenden Verbundkonstruktionen und bei den vorgespannten Konstruktionen das wirkliche Montage-Kräftespiel und die Wirkung der verschiedenen Montagephasen (Stützensenkung, Belastung, Vorspannung usw.) zu beobachten. Diese Aufgabe benötigt eine Messmethode, wo die Messprozesse während der verhältnismässig langweiligen Bauzeit weitergeführt und die Messelemente aufbewahrt werden können. Ausserdem soll die Wirkung der Temperaturänderung beseitigt werden. Bei solchen Aufgaben wurde als Messinstrument der Setzdehnungsmesser Bauart Pfender sehr gut angewendet, der mit einer Messlänge von 100 mm, mit entsprechender Temperaturkompensation, eine Genauigkeit vont 20 kp/cm² sichert. Mit dieser Methode wurde in Ungarn der Bau von zwei durchlaufenden Verbundkonstruktionen in der Bauzeit durch mehrere Monate ständig kontrolliert.

Literatur

[1] Hartmann-Melan: Der Brückenbau. Franz Deuticke Verlag,
           Wien, 1951.

[2] Tóth-Visontai: Statische Messungen an der Strassenbrücke
           über die Theiss bei Tiszafüred.
           Periodica Polytechnica Vol. 13. No 3-4.
           Budapest 1969.

[3] Cornelius: Über den Einfluss der Torsionssteifigkeit auf die
           verdrehung von Tragwerken. MAN-Forschungsheft,
           Augsburg, 1951.

[4] Kristóf-Szittner: Dynamische Untersuchungen an der Tisza-
           Strassenbrücke bei Tiszafüred.
           Periodica Polytechnica Vol. 13. No 3-4.
           Budapest 1969.

[5] Frage D 23. Ermittlung der dynamischen Beanspruchungen von
           Brücken. Bericht über den Vorversuch an der Rhone-
           brücke Riddes der SBB.
           UIC-ORE, Utrecht, 1957.

Zusammenfassung

Der Lehrstuhl für Stahlkonstruktionen der TU Budapest hat
an verschiedenen neugebauten Stahlbrücken Kontrollmessungen
durchgeführt. Mittels dieser Messungen wurden die auf theoreti-
schem Grunde gerechneten Werte des Kräftespieles, der Querver-
teilung, der Torsionssteifigkeit, der Knotenpunkt-Nebenspannun-
gen, das dynamische Verhalten der Strassenbrücken und das Kräf-
tespiel in verschiedenen Bauphasen kontrolliert. Der Diskussions-
beitrag gibt einen Überblick über die Messmethoden und die Er-
gebnisse.

Leere Seite

Blank page

Page vide

Actual Traffic Loadings on Highway Bridges and Stress Levels in Bridge Members

Charges de trafic actuel sur ponts-routes et niveaux de sollicitations dans les membrures des ponts

Gegenwärtige Verkehrslasten auf Strassenbrücken und Beanspruchungs-Niveau in Brückenelementen

EIICHI MURAKAMI
Director
Honshu-Shikoku Bridge Authority

TETSUO KUNIHIRO
Chief, Bridge Section
Public Works Research Institute
Ministry of Construction

MINORU OHTA
Deputy Chief, Second Design Room
Honshu-Shikoku Bridge Authority

HAJIME ASAKURA
Research Engineer, Bridge Section
Public Works Research Institute
Ministry of Construction

Japan

1. Introduction

The design live load specified in the design specifications for highway bridges in Japan, as shown in Fig. 1 and Fig. 2, is fundamentally based on a 20 ton truck and traffic rows composed of a 20 ton truck and 15 ton trucks. The T-load in Fig. 1 is used for design of slab and floor system, while the L-load shown in Fig. 2 is used for design of main girder and main truss. These loads have been used since 1956, but the increase in both weight and number of trucks in these years is so remarkable that the loads shown in the current specifications have reached the state which may not be necessarily appropriate in contrast with the actual traffic situation. Besides, there exist a great number of old bridges which were designed for smaller load, than that of current specifications, and the safety of those bridges under the present heavy load is posing a problem.

In Japan, various surveys of actual traffic loadings and stress levels in highway bridge members are being carried out for the purpose of obtaining the data in re-examination of design live load, and also for control of safety of existing bridges.

2. Stress levels in bridge members[1]

Stress levels caused in the main girder of 18 plate girder bridges (with span length of 20 to 60 m) and for each member of a truss bridge (with span length of 80 m) under the ordinary traffic loading were measured.

In measuring, the device enabling to automatically count up the frequency by each stress level separately was used. This device is composed of the strain detector in which differential transformer is used and recording device which classifies the detected strain separately by four class levels, and count up the respective frequency.
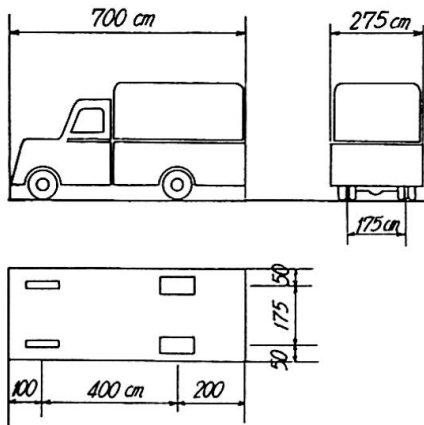
Fig. 1 T - load

Total weight   20 ton
Weight of front wheel 2 ton
Weight of rear wheel   8 ton
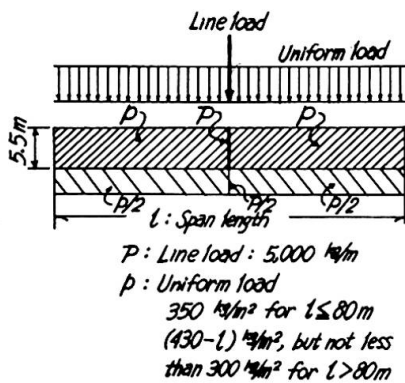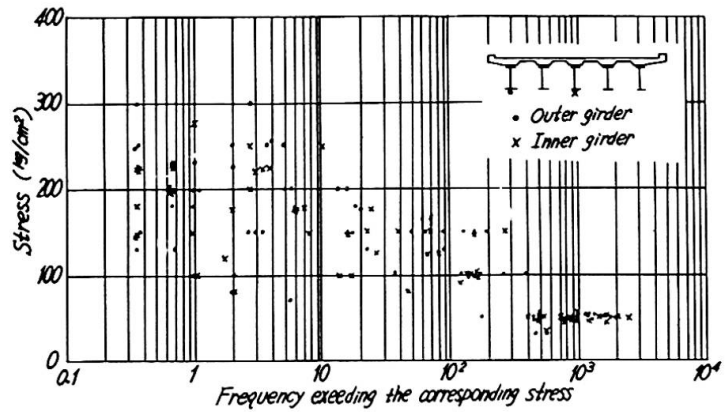
Fig. 3 Stress frequency (Plate girder bridge)

Fig. 2 L - load

P : Line load : 5,000 kg/m

p : Uniform load
  350 kg/m² for $l \leq 80m$
  (430-l) kg/m², but not less than 300 kg/m² for $l > 80m$
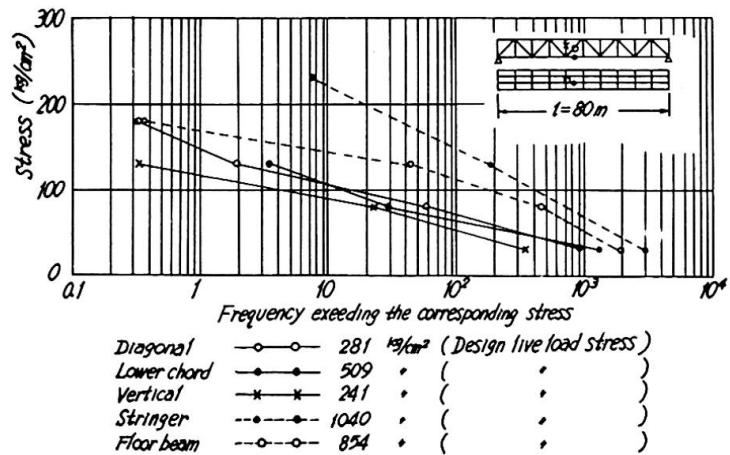
Fig. 4 Stress frequency (Truss bridge)

Diagonal	—o—o—	281 kg/cm² (Design live load stress)
Lower chord	—•—•—	509 ,, (,,)
Vertical	—x—x—	241 ,, (,,)
Stringer	--•--•--	1040 ,, (,,)
Floor beam	--o--o--	854 ,, (,,)

Type of Vehicles	Passenger Car	Bus	Small Size Truck (Gross Weight of 7.5 ton or less)	Large Size Truck (Gross Weight of 7.6 ton or more)	Total
Ratio (%)	67.9	18.1	1.5	12.5	100

Table 1. Percentage of various vehicles

The bridges for which the survey was made were selected from those which are located on the main national highways served for heavy traffic. The traffic amount per 24 hours at the survey point counts 10,000 to 40,000 vehicles, and the average traffic volume for the entire survey points was about 20,000 vechicles, the percentage of various types of vehicles being as shown in Table 1.

The measurement was curried out for 3 to 5 consecutive days. The result of measurements for plate girder bridges and a truss bridge are indicated in Fig. 3 and Fig. 4, respectively. In those

figures, the frequency at each stress level is shown per one day (24 hours). The relation between the range of the ratio of stress level measured in girder bridges to the calculated stress due to the current design live load (L-load) and the frequency caused per the traffic volume of 10,000 vehicles is shown in Fig. 5.

In the case of truss bridge shown in Fig. 4, the values of measured stress of floor system is greater than those of truss members. However, the ratio of measured stress level to design live load stress for floor system is smaller than that of truss members. This is supposed to be due to the fact the reinforced concrete slab supported by the stringers and floor beams may take charge a portion of the function of stringers or floor beams. Such a function of reinforced concrete slab was not considered in the design calculation.

According to the fact mentioned above, it is known that the live load stress caused in each member of bridge under ordinary traffic load is some 300 kg/cm^2 at most, which is fairly at lower level as compared with the calculated stress level due to design live load.

3. Actual status of wheel load[2)3)]

For the purpose of confirming the actual weight of wheel load of vehicle having great influence on the slab and floor system, measurement of weight of wheel load was carried out at 34 points on national highways in Japan.

The device used for the measurement is composed of weighing part and recording part. The weighing apparatus is the weighing meter consisting of a sheet of steel plate and four loadcells
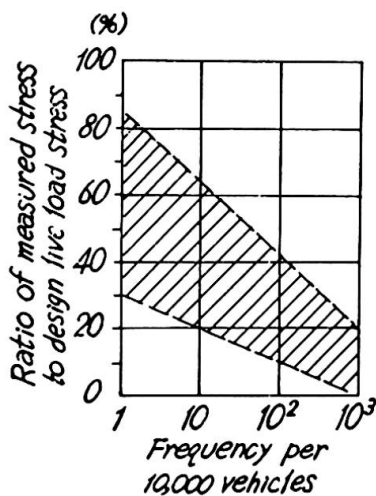

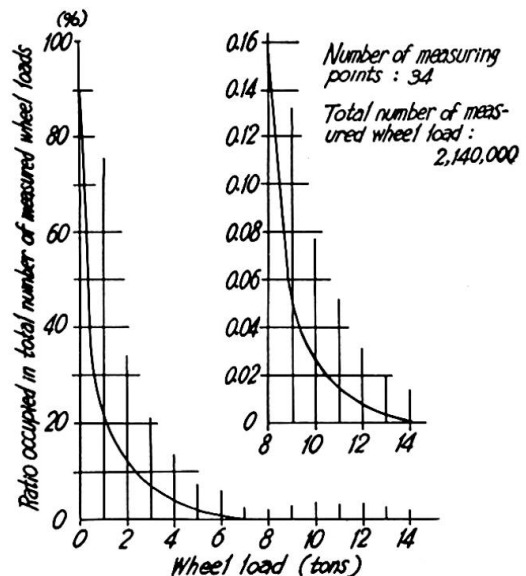Fig. 5 Ratio of measured stress to design live load stress

Fig. 6 Cumulative frequency distribution of wheel load

supporting the plate on its four corners. The weighing meter is
installed in the reinforced concrete pit in such a way that the
loading plate makes a part of the road surface covering the pit,
so that the weight of wheel passing over the plate is detected
without stopping the vehicles. The recording part has the function
of classifying counting automatically each frequency of the
detected weight by every 12 classes of level.

The survey points were selected from among the points located
on main national highway, and besides, where the traffic is
especially crowded. The traffic volume per 24 hours for the lane
where the wheel load was measured indicated about 5,000 vehicles
at point where the traffic volume was the least, and about 28,000
vehicles where the traffic volume was the most.

The measurement was carried out for 1 to 7 days for each
point. It was made clear, as the result of the survey, that the
frequency by different level of wheel load showed considerable
difference according to the survey point, but on the same point,
approximately the same frequency distribution was observed.

Fig. 6 represents the frequency measured by various weight
of wheel load. As known from Fig. 6, although about 80% of the
whole number of wheel load measured is one ton or less, and the
number of heavier wheel load decreases rapidly, the fact that
the number of wheel load exceeding design wheel load of 8 ton
(which is approximately the same as the wheel load of HS20 of
AASHO, see Fig. 1) amounts to 0.16% of whole number of wheel load,
namely, that there exist about 32 vehicles of which wheel load
exceeds design wheel load of 8 ton, per 10,000 vehicles, may not
be ignored from the point of view of design of new bridges or
maintenance and safety of the existing bridges. The reason of
the existence of wheel loads heavier than design wheel load is
due, needless to say, to the operation of large size trucks which
are loaded more than the statutory loading limit.

In Japan, the expansion of truck size has been advanced in
these years to reduce the cost of transportation. At the same
time, the instances of damages of reinforced concrete slab have
become remarkable. As one of the causes thereof, the operation
of vehicles with weight heavier than design wheel load may be
mentioned.

Besides, on account of the fact that the weight and number
of wheel loads of trucks increased, the importance of performing
fatigue design came to be claimed on steel plate deck where
welding is used abundantly. In applying fatigue design, it is
necessary to know the value and number of repetition of stress
imposed during the expected life of bridge. From the point of
view of fatigue, the effect of random wheel loads with different
weights and numbers of repetition on steel plate deck may be
evaluated by means of "equivalent number of repetition" of design
live load stress due to design wheel load (8 ton), denoted by
the following expression:

$$N_{eq} = K_1 \cdot K_2 \cdot N_t \tag{1}$$

Where N_{eq} :   Equivalent number of repetition of design live load
             stress

N_t : Number of total passing wheel loads during the expected life of the bridge

K_1, K_2: Coefficients

K_1 in Equation (1) is the coefficient used for converting the wheel load with certain weight into design wheel load of 8 ton, which may be expressed as Equation (2):

$$K_1 = \sum P(T) \left(\frac{T}{8}\right)^{\frac{1}{k}} \cdot \Delta T \qquad (2)$$

Where T : Weight of wheel load

P(T): Probability of occurrence of T

k : Coefficient determined from S-N diagram (the slope of S-N diagram in logarithmic sclae.)

The position where wheel loads pass in certain traffic lane is not stationary. Fig. 7, illustrated as an example, shows that the distribution of passing positions of wheel loads in a traffic lane may be regarded as a normal distribution with the standard deviation of approximately 35 cm. Fig. 7 was obtained as the result of observation at 20 different points on national highways with two or four lanes, all over Japan. K_2 in Equation (1) is the coefficient to be multiplied with the number of repetition determined on the assumption that the all wheel loads pass on a fixed position, and is given from the following equation:

$$K_2 = \sum \left(\frac{R(x)}{R_0}\right)^{\frac{1}{k}} \cdot P(x) \cdot \Delta(x) \qquad (3)$$

Where Ro : Design live load stress

R(x): Stress of member under the design wheel load passing on certain position, x

P(x): Probability of occurrence of R(x)

The value of K_2 for the longitudinal rib of steel plate deck which is commonly used in Japan, is approximately 0.2.

P(T) in Equation (2) is given by Fig. 6, and P(x) in Equation (3), by Fig. 7. Such data, actually observed concerning the weight and the passing position of wheel load are indispensable for the fatigue design.

4. Actual status of vehicle row load[2],[3]

L-load, shown in Fig. 2, depends upon the vehicle row load such as shown in Fig. 8.
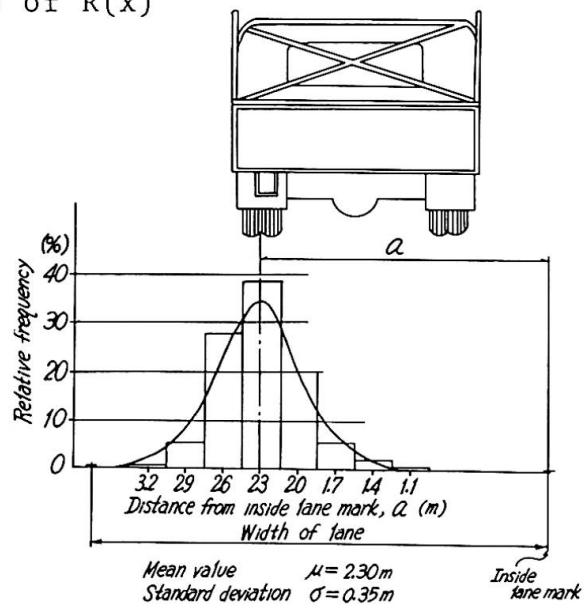
In order to ascertain the magnitude of actual vehicle row

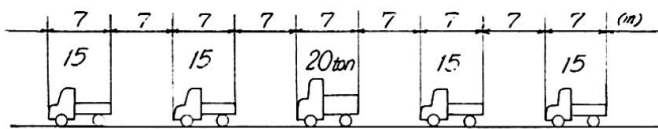Fig. 7 Distribution of passing position of wheel

Fig. 8   Basic traffic pattern of
          L - load

Number of lanes	Number of points
2	25
4	40
6	8
	73

Table 2. Number of traffic pattern survey points

a. Smooth running state (Pattern I)

b. Semi-congested state (Pattern II)

C. Perfectly congested state (Pattern III)
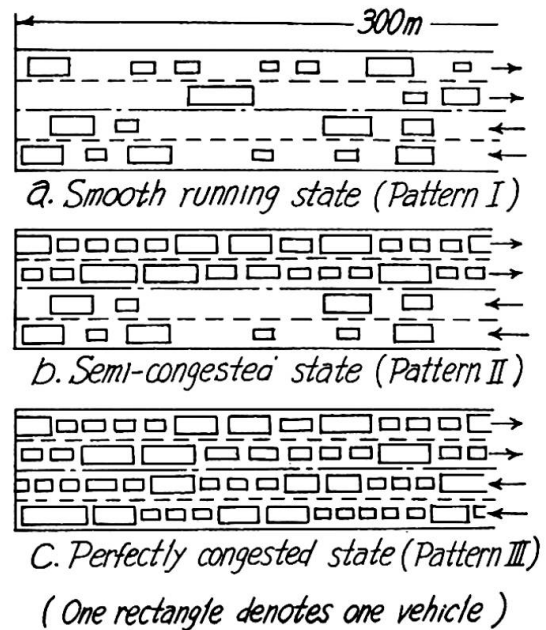
(One rectangle denotes one vehicle)

Fig. 9 Traffic patterns

load in comparison with the above design L-load, a survey on traffic pattern was carried out in the following procedure:

1)   73 survey points were selected (Table 2). These points are the places on the main national highways where the traffic is crowded and apt to be congested including a lot of large size vehicles.

2)   At each survey point, traffic pattern extending over 300 m on the roadway was photographed intending to take as many heavy trucks as possible in the overlooked picture. Ten times of the photographing was carried out, and selected one case of pictures which appeared to be most congested in traffic, as they were assumed to represent the maximum of vehicle row load at the point.

3)   Distinguishing the loading condition of each vehicle with or without cargo, as well as the type of each vehicle from the photograph, the figure of traffic pattern (Pattern I), as illustrated in Fig. 9a, which shows exactly same arrangement of vehicles as on the photograph was prepared. For the weight of different types of vehicles and different loading conditions, corresponding average values were established referring to the table of size and weight of motor vehicles in Japan.

4)   On the basis of Pattern I, hypothetic pattern such as Fig. 9b (Pattern II) in which the half of traffic lanes is congested, while the opposite half lanes is smooth, and Fig. 9c (Pattern III) in which the whole lanes are perfectly congested, were prepared. In this case, the clear distance between two consective vehicles in the congested state was taken as 1 m, with reference to the vehicle distance observed on highways actually at the time of congested. Pattern II is the state which is usually observed in Japan, and Pattern III is the state which is very rarely observed.

5)   In regard to Pattern I, II and III, the maximum bending moment Mo and maximum shear force So, which are imposed in a simply supported girder under each loading pattern, were calculated by means of electronic computer.   In this case, Mo and So were obtained for nine cases of the span length of 20, 40, 60, 80, 100, 150, 200, 250 and 300 meters.

6)   M/M_D and So/S_D were calculated, which are the ratio of Mo and So due to "actual vehicle load" obtained in 5), to beinding moment M_D and shear force S_D due to "design load" showed in Fig. 2.

a. PATTERN-I (Smooth running state)

b. PATTERN-II (Semi-congested state)
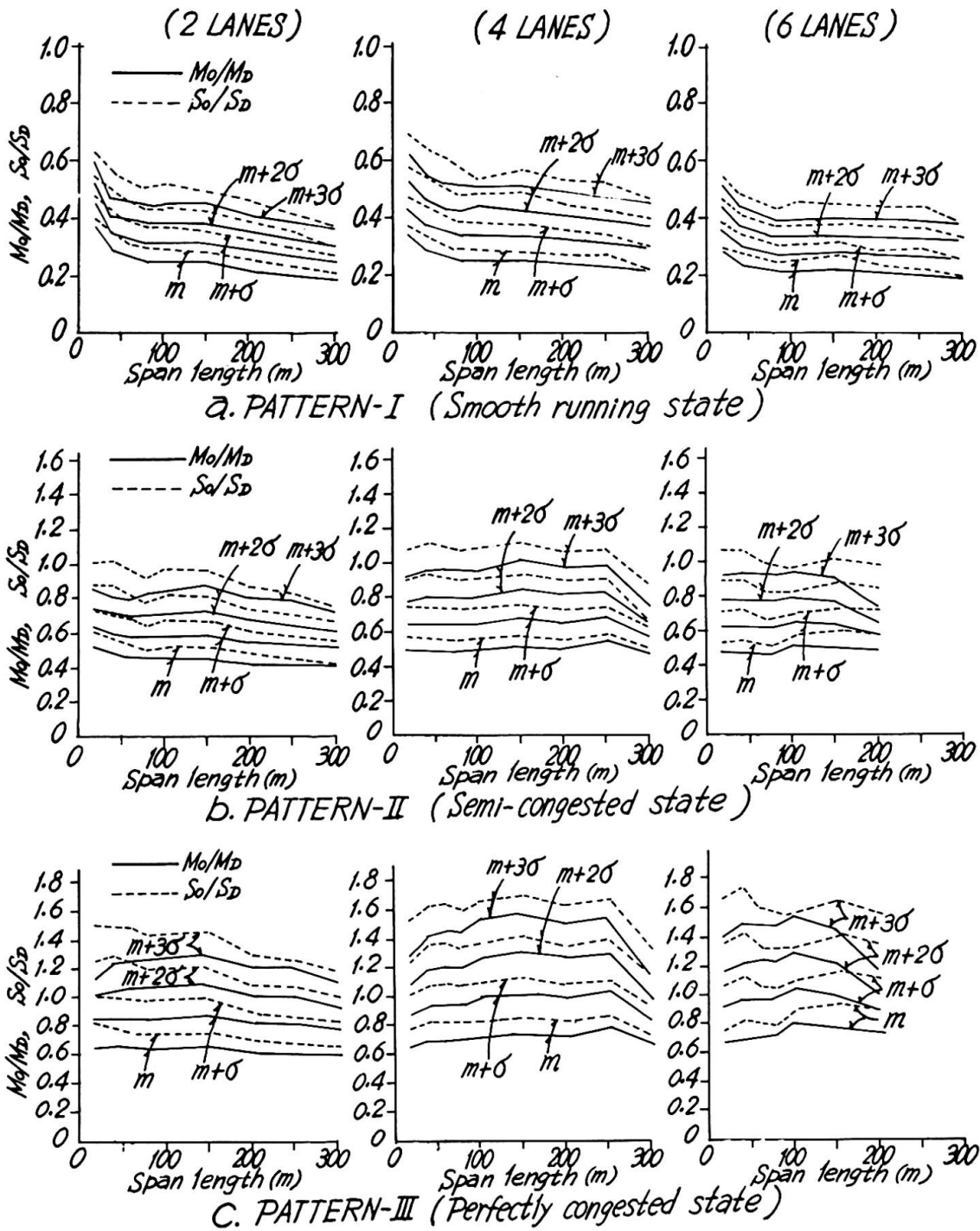
C. PATTERN-III (Perfectly congested state)

Fig. 10   Ratio of measured value to calculated value due to design load

The values of Mo/M_D and So/S_D thus obtained for all of observed points were gathered up for different number of lanes, and a histogram of Mo/M_D and So/S_D was drawn. The histogram showed that the form of distribution of Mo/M_D and So/S_D may be regarded as the normal distribution. Thereupon, the mean value "m" and the standard deviation "σ" of the values of Mo/M_D and So/S_D for different numbers of traffic lane and for different span lengths were calculated, then the relation between different expected magnitudes of the vehicle row load and their frequencies was presumed.

Fig. 10 was obtained in this way, indicating the features of magnitude of actual vehicles load in Japan. From Fig. 10, the following facts may be understood:

1)   The magnitude of vehicle row load under normal traffic condition (Pattern I) is considerably low, the average value of the loading effects (moment and shear) in main girder is equal to 30%, at most, of those due to design live load regardless of the number of traffic lane and of span length, and even at the level of $(m+3\sigma)$, it is only 60%, at most, of the loading effects due to design live load.

2)   Under the semi-congested state of traffic (Pattern II), that is usally occured in Japan, the average value of the loading effect imposed in main girder ranges from 40 to 60% of that due to design live load, and the level of $(m+3\sigma)$,corresponds approximately to the level of design live load.

3)   When vehicles are congested with clear distance of 1 m over the whole lanes (Pattern III), the average value of loading effect imposed in main girder is presumed to be 60 to 80% of that due to design live load, and the level of $(m+\sigma)$ corresponds approximately to the level of design live load.

4) So/S_D is usually larger than Mo/M_D. Namely, the current design live load in Japan is not well-balanced between bending moment and shearing force in main girder.

Fig. 11, comparison of loading effects due to design live load of well-known HS 20 Loading of AASHO (1969) and "Brücken Klasse 60" of DIN 1072 (1967) to those due to Japanese design live load, may facilitate understanding the consideration made in this report.
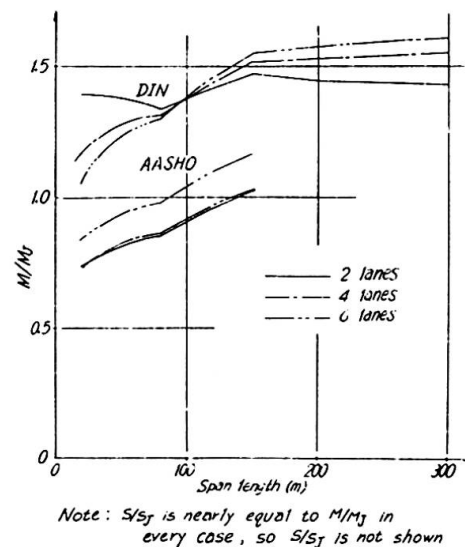

Note : S/S_J is nearly equal to M/M_J in every case, so S/S_J is not shown

Fig. 11   Comparison of design loading effect in various countries

5. Conclusion

The following conclusion may be introduced concerning the load on highway bridges in Japan, on the basis of the results measured on the stress levels in bridge members, and on the wheel load and vehicle row load:

1)   The live load stress imposed in main girder and main truss under usual traffic condition is 300 kg/cm^2 or so at most, which is considerably small as compared with the calculated design live load stress.

2)   Vehicle row load under normal traffic condition is in considerably lower level as compared with the current design vehicle row load, but under the state in which the whole lanes are perfectly congested, there is a little chance that the vehicle row load may reach to the level of design load. Considering the fact that semi-congested state of traffic in which the half of traffic lanes are congested while the opposite half lanes are smooth is usually observed wherever in Japan, it seems to be suitable to determine the design load for main girder on the basis of such loading condition.

3)   The relation between the weight and frequency of vehicle wheel load shows fairly big divergence according to area, but nearly constant trend on the same point. Generally speaking, the actual condition of wheel load is that it has no such allowance to design load as is seen in the vehicle row load, and the existence of such heavy wheel load exceeding design wheel load is amounting to a number which may not be ignored.

4)   Since vehicle wheel load (single vehicle load) is in the severer condition than in the case of vehicle row load in comparison with the current design load, considerable unbalance of load carring capacity between main girder and floor system has been arisen. In order to design a bridge of which each member is well balanced in strength, it will be necessary, so long as the current design load is employed, to use larger safety factor for the floor system than that for main girder.

References

1) Tetsuo Kunihiro, Minoru Ohta: "A Study on Stress Levels on Highway Bridges", Annual Meeting of Civil Engineering, Ministry of Construction, 1968 and 1969. (In Japanese)

2) Tetsuo Kunihiro, Minoru Ohta: "A Study on the Actual Condition of Traffic Load and its Effect on Highway Bridges", Report of Public Works Research Institute, Ministry of Construction, No. 626, Oct. 1970.(In Japanese)

3) Tetsuo Kunihoro, Hajime Asakura and Keiichi Inoue: "Study on Design Live Load", Report of Public Works Research Institute, Ministry of Construction, No. 701, Nov. 1971. (In Japanese)

Summary

     As the result of our surveys of wheel load, row load of
vehicles and of stress in bridge members, it was made clear that
the magnitude of vehicle row load or corresponding stress in main
girder has considerable allowance in comparison with the current
design live load and corresponding stress, under any traffic
loading condition except perfectly congested states, while the
single vehicle load sometimes exceeds the design load and poses
a problem in relation to the safety of slab and floor system.

Mesure des variations de réactions d'appuis d'ouvrages hyperstatiques en béton précontraint ou mixtes

Messungen von Variationen von Auflagerreaktionen bei statisch unbestimmten, vorgespannten oder Verbundbauwerken

Measuring of Variations of Support Reactions at Undetermined Prestressed or Mixed Structures

S. BRETONNIÈRE   M. DIRUY
Laboratoire Central des Ponts et Chaussées
Paris, France

1. INTRODUCTION

L'étude expérimentale du comportement à long terme des ouvrages présente nombre de difficultés, eu égard aux techniques délicates de mesures in situ qu'elle implique. En ce qui concerne les ouvrages hyperstatiques, la mesure permanente des réactions d'appuis constitue un puissant moyen d'étude de la redistribution des contraintes due aux phénomènes à long terme imputables à la nature des matériaux constituants, à leur rhéologie (retrait et fluage du béton, relaxation des câbles de précontrainte) ainsi qu'aux variations climatiques environnantes (hygrométrie, température, ensoleillement).

De telles mesures nécessitent des capteurs devant répondre à des critères très particuliers :

- grande sensibilité, les variations de force à mesurer étant parfois très faibles par rapport à la charge permanente,

- absence totale de dérive, l'évolution des réactions devant pouvoir être suivie à très long terme,

- insensibilité aux sollicitations diverses d'ordre thermique ou mécanique (mouvements relatifs tablier-appui).

Les dynamomètres à déformation élastique présentent une dérive due au fluage du corps d'épreuve qui ne peut être éliminée que par une reprise périodique du zéro du capteur. Cette opération dans le cas des appuis de pont nécessite le déchargement du dynamomètre par un dispositif spécial reprenant les efforts. L'influence des sollicitations perturbatrices, mécaniques ou thermiques, est également difficile à éliminer d'où la mise au point d'un nouveau procédé qui utilise une cellule de charge ayant les qualités requises.
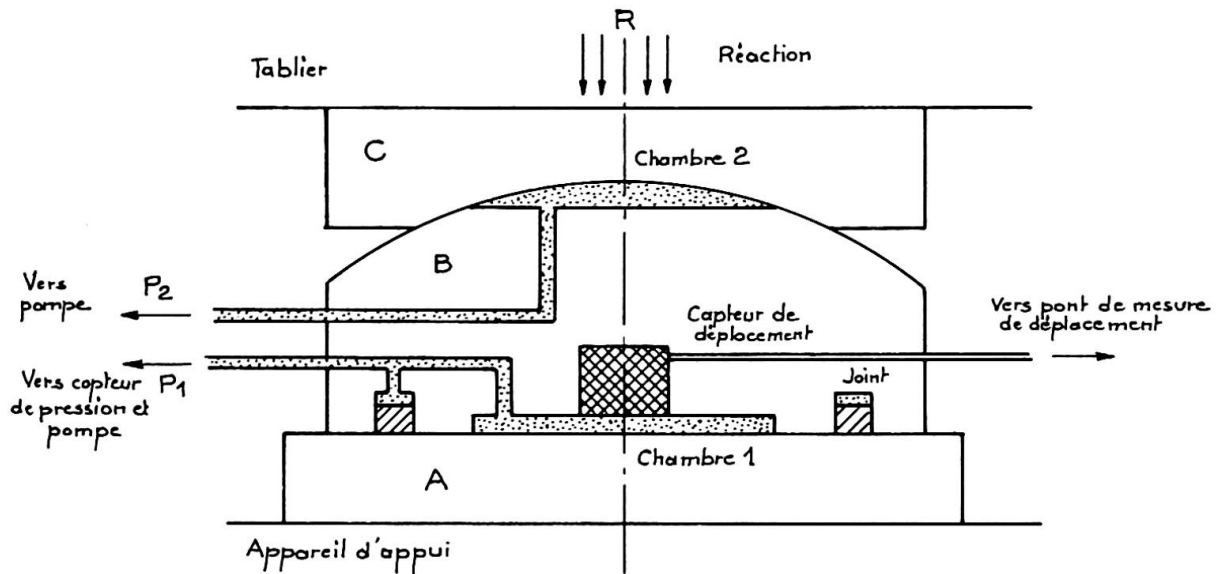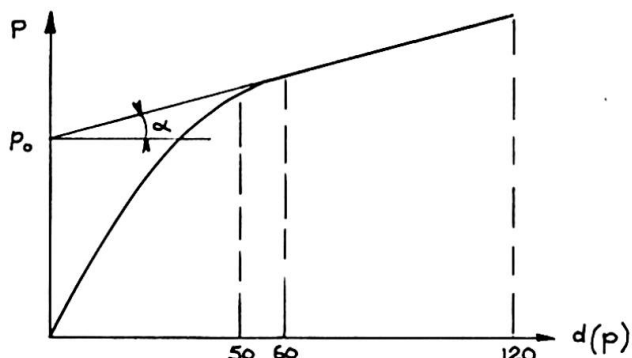
2. PRINCIPE DE LA CELLULE DE CHARGE

Fig. 1 – Schéma de fonctionnement

La cellule de charge directement interposée entre l'appui de l'ouvrage et le tablier, est constituée par 3 blocs rigides superposés (voir fig. 1 ci-dessus).

Ces blocs sont en contact par des faces planes rectifiées (A et B) ou par des surfaces sphériques (B et C). Deux chambres ménagées dans B peuvent être alimentées indépendamment sous pression d'huile au moyen d'une petite pompe à main.

La pression dans la chambre 1, développe à partir d'une certaine valeur une force qui équilibre la réaction d'appui et entraîne le soulèvement de B. Le déplacement relatif "d" de A et B, mesuré par un capteur incorporé à la cellule, est fonction de la pression hydraulique mesurée par un capteur indépendant de la cellule. Il faut atteindre un écartement de 50 à 60 μ pour éliminer tout contact entre B et C et obtenir, pour des déplacements inférieurs à 120 μ , une variation linéaire de p en fonction de d. La pente (α) de cette droite, traduisant la rigidité de l'ouvrage, est obtenue par des mesures de p de 10 μ en 10 μ . La pression p_o pour d = 0, obtenue par extrapolation, fournit d'après la courbe d'étalonnage la valeur de la réaction d'appui.

Fig. 2 –   p = f (d)

Toutefois le fonctionnement correct du dynamomètre n'est assuré que si la réaction d'appui R est centrée sur la chambre 1 sans aucun moment entre les blocs A et B. Dans ce but, avant toute mesure, la chambre 2 est mise sous pression d'huile pour permettre à l'élément C de rotuler sans frottement sur coussin d'huile.

3. CARACTERISTIQUES METROLOGIQUES

La force maximum mesurable avec une cellule de charge est fonction de la pression admissible dans la chambre et de sa surface.

La pression normale de service est de 250 bars et peut atteindre exceptionnellement 400 bars, ce qui permet de réaliser des cellules pour des forces de plusieurs centaines de tonnes.

Les erreurs de linéarité dues à la cellule de charge proviennent des variations possibles de la surface efficace de la chambre 1 ; le montage particulier du joint d'étanchéité permet de limiter cette erreur à 0,2 % pour des variations de pression comprises entre 2 bars et 400 bars.

La fidélité est très bonne et le pouvoir de résolution inférieur à 5.10^{-4} de la force mesurée. La cellule ne présente aucune hystérésis mesurable (vérifié lors d'étalonnage au 1/1000è près en laboratoire sur des cellules de force 100 KN).

Des variations de température entraînent des modifications de la section efficace de la chambre de l'ordre de 0,1 % pour $\Delta T = 40°C$.

La précision des mesures est étroitement liée aux caractéristiques de la chaîne de mesure de pression qui peut être réétalonnée fréquemment. Pour des domaines de variation de force très étendus pouvant entraîner des variations de pression comprises entre 1 bar et 400 bars, il est nécessaire d'utiliser plusieurs capteurs d'étendues de mesure différentes. Dans le cas des réactions d'appuis les variations excèdent rarement ± 15 % et la pression nominale du capteur est donnée en conséquence.

Ce procédé peut fournir la valeur des réactions d'appui avec une précision inférieure à ± 0,2 % à condition de disposer des moyens d'étalonnage en force.

4. UTILISATION PRATIQUE

Pour effectuer les mesures deux opérateurs sont nécessaires, l'un pour imposer la pression d'huile en fonction des déplacements désirés, l'autre pour mesurer cette pression grâce à un capteur à jauges de déformation et un pont de mesure statique de haute précision.

Pour les mesures de réactions d'appui, où chaque extrémité de travée est équipée de deux cellules de charge, on relève successivement les valeurs. Dans ces conditions la pente de la partie linéaire de la courbe p = f (d) est surtout liée à la rigidité de torsion de l'ouvrage, la rigidité de flexion intervenant très peu.

5. APPLICATIONS

5.1 Modèle de pont mixte

Une ossature mixte acier-béton a fait l'objet d'une étude ré-
cente comportant notamment une série de mesures à moyen terme
(quelques mois) ayant pour but une meilleure connaissance des effets
du retrait de la dalle de béton sur le comportement de l'ouvrage. Ce
dernier, construit dans le hall d'essais du Laboratoire Central des
Ponts & Chaussées comportait 2 travées de 9,5 m (voir schéma fig. 3).
Il reposait sur 6 appuis par l'intermédiaire de 6 pesons hydrauli-
ques de capacité 100 KN (10 T) (photo de la fig. 3). Plusieurs
sections étaient en outre équipées par divers moyens de mesures :
jauges à fil résistant, extensomètres mécaniques et optiques, son-
des de température, dispositifs optiques de mesure des flèches. Des
dalles témoins constituées du même béton que celui du modèle
devaient permettre de mesurer le retrait libre du matériau pris seul.
Les mesures ont débuté en même temps que le coulage de la dalle. Les
courbes de la fig. 4 résument les mesures de réactions d'appuis
effectuées d'abord à intervalle très rapproché (1 h pendant la prise
du béton) puis quotidiennement, ceci pendant 3 mois. La température
et l'hygrométrie ambiantes furent maintenues sensiblement constan-
tes pendant toute cette période ($t = 21° \pm 2$ $H_r = 60 \% \pm 10 \%$). Les
pesons étaient disposés de la façon suivante :

pesons 1 et 4 - appui extrémité gauche

pesons 5 et 6 -   "   "   droite

pesons 2 et 3 -   "   central

On pouvait vérifier le poids du modèle (constant aux pertes
d'eau du béton près) en faisant la somme des réactions d'appuis
après chaque mesure.

Le calcul des réactions hyperstatiques effectué à partir des
mesures extensométriques est en parfaite concordance avec les
réactions mesurées à l'aide des pesons hydrauliques. On remarque
pendant la prise du béton l'influence des phénomènes thermiques
différentiels sur les réactions d'appuis. La perte de poids due au
décoffrage apparaît également ainsi que les charges additionnelles
qui furent ensuite ajoutées aux extrémités de l'ouvrage pour com-
penser un délestage trop important de ces appuis dû au retrait, et
qui risquait d'annuler les réactions d'extrémité.

Par exploitation conjointe des valeurs des réactions d'appuis
et des déformations mesurées, on a pu suivre l'évolution de divers
paramètres, notamment celle du coefficient d'équivalence $\left(n = \dfrac{E_A}{E_B} \right)$
et du retrait libre (ε_r).

A la suite de ces essais il a été procédé à une dénivellation
de l'appui central et à l'étude du fluage-relaxation consécutif.
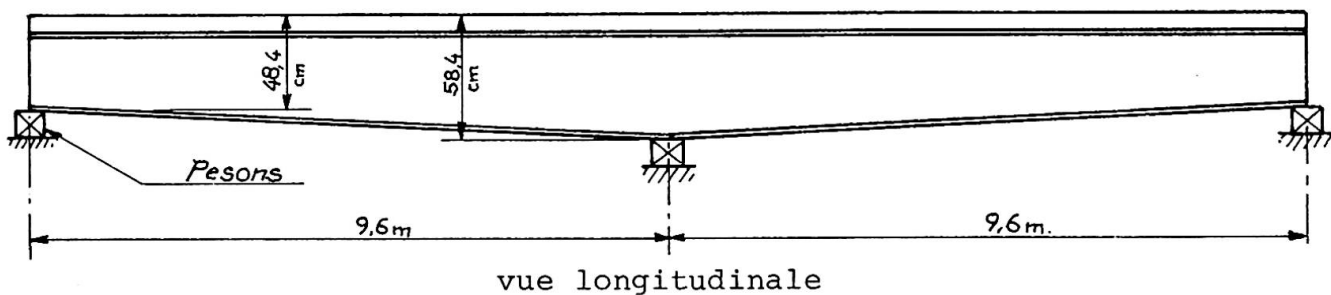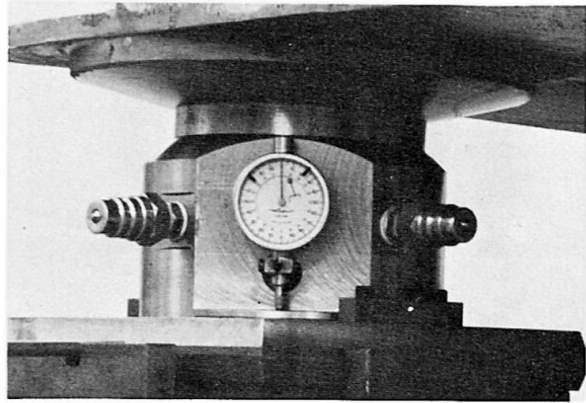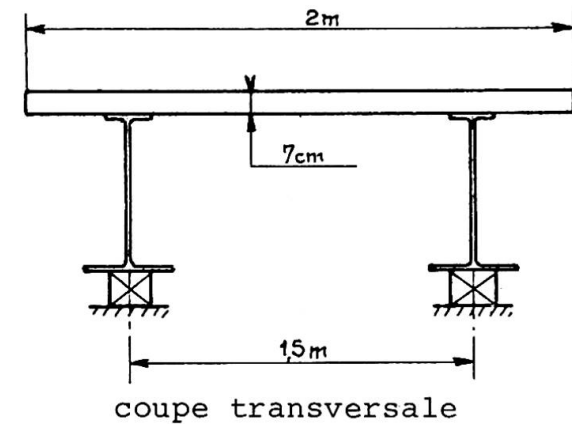L'interprétation des mesures est en cours.

coupe transversale

peson de 100 KN

vue longitudinale

Fig. 3 - Essais d'une ossature mixte acier-béton

5.2 Ponts hyperstatiques en béton précontraint

5.2.1 Pont de Champigny-sur-Yonne

Ouvrage à 3 travées continues de 35 - 70 - 35 m de hauteur constante (voir fig. 5). Fin de construction : Avril 1970. Les culées de cet ouvrage ont été équipées chacune par 2 pesons hydrauliques de capacité 1000 KN (100 T), situés entre le tablier et les appuis néoprène-téflon. Les mesures qui ont été entreprises aussitôt après construction et sont poursuivies actuellement ont pour but principal de contribuer à l'étude de la redistribution des contraintes dues aux phénomènes de retrait-fluage-relaxation dans l'ouvrage. Elles sont effectuées une fois par mois environ. Les variations des réactions d'appuis mesurées sont modulées par les variations journalières de la température du béton. Celles-ci sont surtout dues à l'ensoleillement qui provoque un gradient thermique entre les parties supérieure et inférieure du tablier ; ce gradient amène une déformation différentielle des fibres longitudinales des hourdis et des âmes d'où variations de courbure de l'ouvrage et redistribution des réactions entre les piles et les culées. Le calcul des variations de réactions imputables à ce phénomène thermique est possible si l'on connaît la distribution des températures dans une section. On a donc placé convenablement des sondes thermiques qui renseignent à chaque instant sur la température du béton et permettent d'établir des corrections aux mesures de réactions sur culées.

Les courbes de la fig. 5 résument les mesures déjà effectuées. Après correction les courbes présentent une allure assez régulière

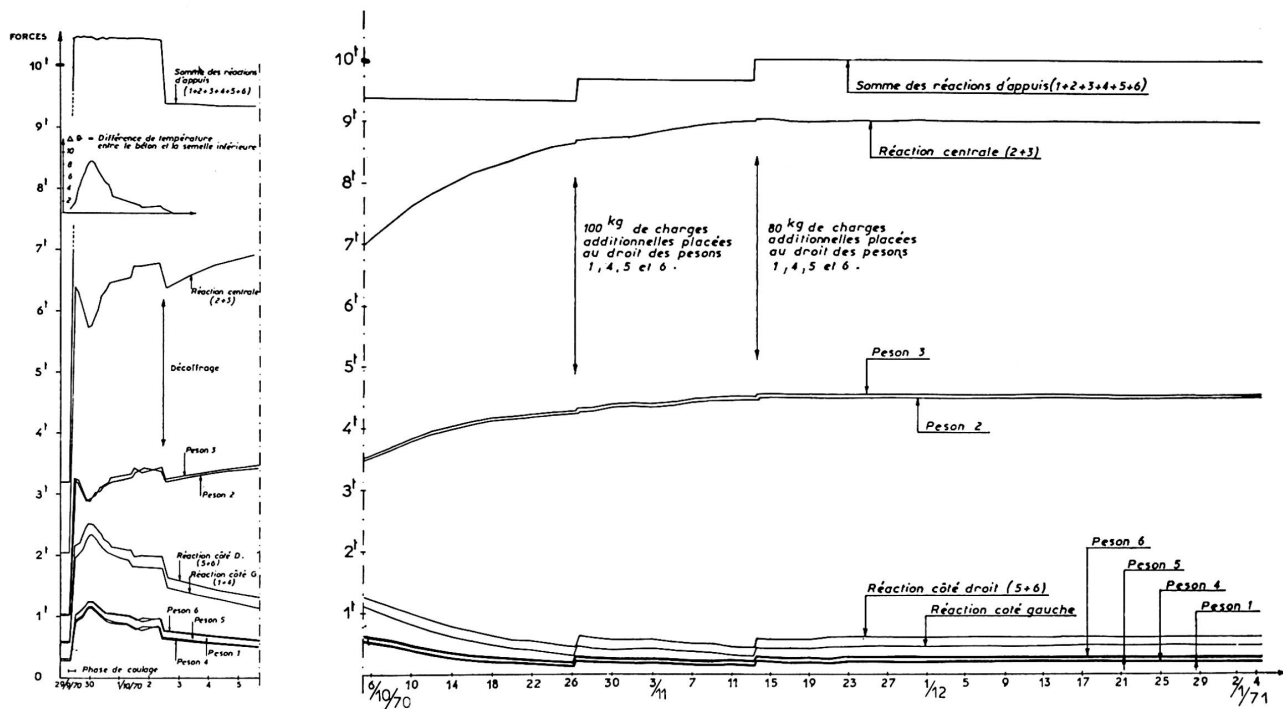. fig 4. Modele de pont mixte - Etude du retrait

Evolution des reactions d'appuis

vue longitudinale

effet de l'ensoleillement

coupe transversale
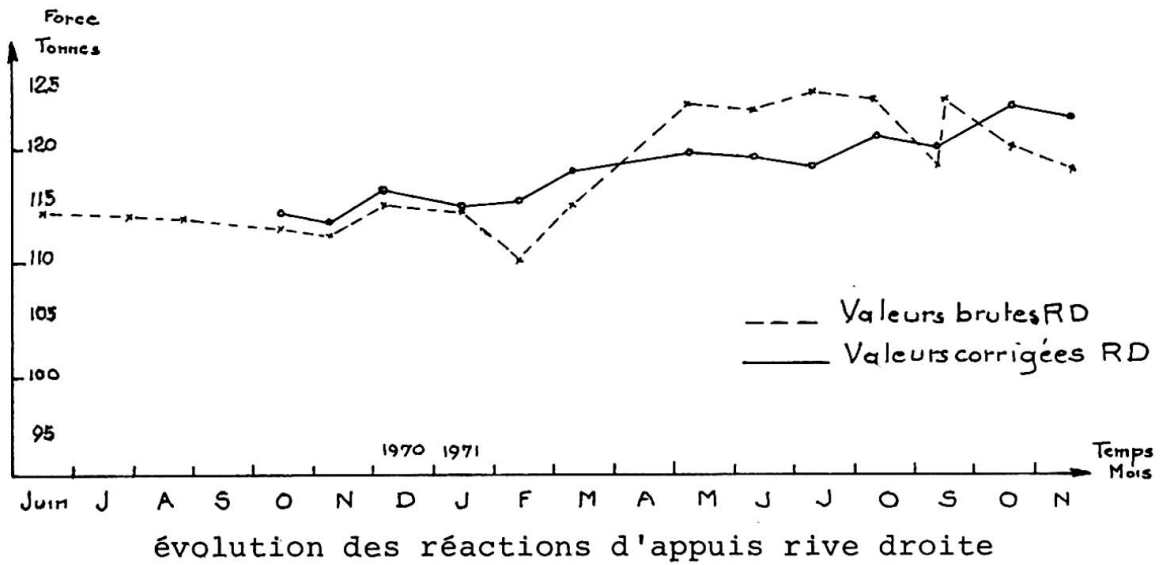du tablier

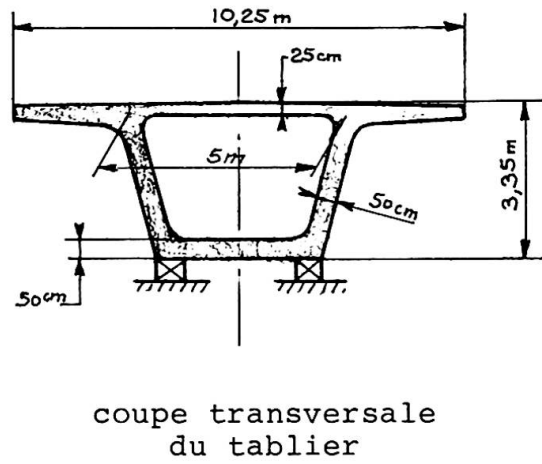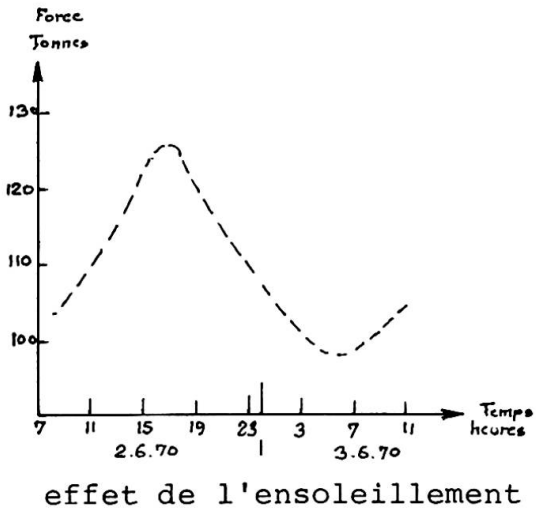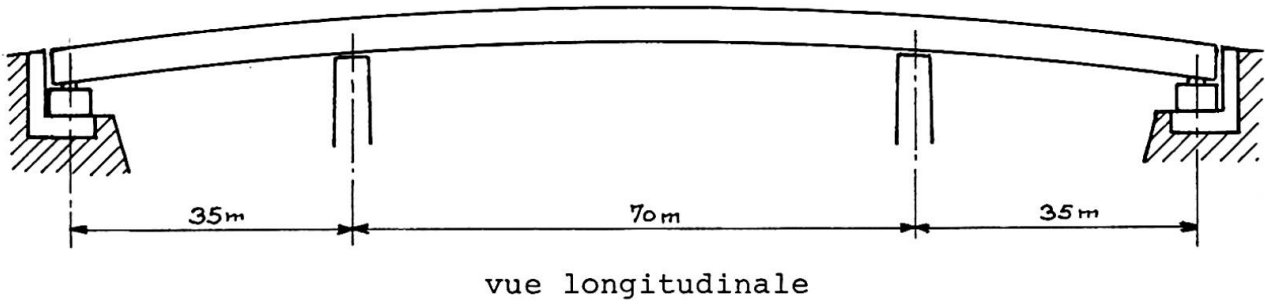évolution des réactions d'appuis rive droite

Fig. 5 - PONT DE CHAMPIGNY S/YONNE

ascendante (8 tonnes pour 1 an) qui peut être due à l'adaptation de
l'ouvrage par fluage relaxation. L'interprétation de ces résultats
ne fait que débuter et ne sera sérieusement engagée que lorsque
les mesures auront été faites sur un laps de temps suffisant (2 ans
environ).

Parallèlement, l'influence de l'ensoleillement sur l'ouvrage a
été étudiée par des campagnes de mesures continues s'étendant sur
24 heures au moins. Au cours de l'une de ces campagnes des varia-
tions de 24 % de la réaction sur culée ont été constatées (fig. 5).
Il s'agit probablement d'un cas extrême pour cet ouvrage mais des
variations journalières de 15 ou 20 % sont courantes l'été. De
telles constatations incitent assurément à la réflexion car l'ou-
vrage de Champigny n'est pas exceptionnel par sa situation géogra-
phique et nombre d'ouvrages de même type doivent subir des condi-
tions climatiques plus sévères.

5.2.2   Pont de Tourville (sur la Seine)

Une étude analogue à celle concernant le pont de Champigny a
été récemment entreprise sur un ouvrage en Béton Précontraint à 3
travées continues de 60 –90 –60 m , mais d'inertie variable.

Des pesons hydrauliques sont disposés sur les culées et la
réaction par culée est de l'ordre de 2000 KN. Les mesures ont
débuté en Mai 1971 et il est trop tôt pour en donner des résultats
intéressants.

RESUME

Un dynamomètre hydraulique très sensible, sans dérive, et de
haute fiabilité a été mis au point pour les mesures de réactions
d'appuis des ouvrages.

Deux types d'applications en ont été faites :

1) Modèle de Pont Mixte étudié en hall d'essais –

   Etude du retrait de la dalle de béton et des effets d'une
   dénivellation d'appuis.

2) Ouvrages en béton précontraint : Champigny-sur-Yonne et
   Tourville.
   Etude de la redistribution des réactions d'appuis due à
   l'adaptation par fluage-relaxation de l'ouvrage.

   Etude de l'influence des gradients thermiques sur la valeur
   des réactions d'appuis.

Aerodynamic Behaviour of the Cable Stayed Bridge Toyosato Ohhashi

Comportement aérodynamique du pont haubané de Toyosato Ohhashi

Aerodynamisches Verhalten der seilabgespannten Toyosato-Ohhashi-Brücke

I. KONISHI
Prof. Dr.
Department of Civil Engineering
Kyoto University, Japan

S. KOMATSU
Prof. Dr.
Department of Civil Engineering
Osaka University, Japan

H. INOUE
Chief of Bridge Department
Osaka City, Japan

Abstract

This paper describes the aerodynamic behavior of a cable-stayed girder bridge. The wind tunnel experiment was conducted at relatively large Reynolds numbers by using a sectional model, which was 1/20 scale of a prototype.

The results show that the cable-stayed girder bridge with a trapezoidal closed cross section is always stable against a horizontal wind. However, some restricted motions could occur in an inclined wind to a horizontal direction with a comparatively low wind velocity and not so large amplitudes.

To make clear the aerodynamic behavior of the prototype in turbulent flow, the observation of atmospheric turbulences at the site where the prototype was constructed has been continued. By analyzing the structures in the atmospheric turbulence, it was recognized that the restricted motions, which had been observed in the wind tunnel experiment by using a smooth flow, would not occur in the prototype which was subjected to a natural wind fluctuating at random.

1   Introduction

The authers have been concerned about the response of flexible structures to a wind. Such structures as suspension bridges, tall stacks and cable-stayed girder bridges are known to be vulnerable to the effect of a wind. It has been known that a large number of bridges and stacks were damaged or destroyed by winds. Especially, the failure of the Tacoma Narrows Bridge which is a suspension bridge having a main span 853 meters long is known to be a remarkable accident. This bridge was destroyed by twisting vibrations which occurred at a relatively low wind speed of 19 m/s. After this accident, many treaties on aerodynamic behaviors of suspension bridges were presented.

F. Bleich[1]) suggested that the aerodynamic instability of suspension bridges showed a flutter as experienced with the wings, and applied to the suspension bridges the general theory previously applied to an aeroplane by Theodorsen and others. Many studies have been done since Bleich presented his report. According to the fact that in most cases suspension bridges have complex cross sectional shapes compared with wings, experimental values can not agree well with the theoretical results.

Recently, G. V. Parkinson[2]) has suggested that a gallopping oscilation of a

prismatic bar is to be considered as a nonlinear self-exited oscilation. And he stated that this theory well fit the experimental result for bluff cross section like The Tacoma Narrow Bridge.

The above-mentioned studies are mainly concerned with the aerodynamic stability of suspension bridges in a smooth flow. On the contrary, it has been pointed out that the effect of a turbulence of a natural wind must be considered. A. C. Davenport[3] has applied a noise theory to determine the response of a suspension bridge in a turbulent flow.

The aerodynamic behavior of a bridge is different from each other, because it has different cross sectional shape, dimensions and dynamic characteristics. So, none can predict exactly its behavior without carrying out a wind tunnel experiment.

The authers conducted a wind tunnel experiment to investigate the aerodynamic stability of a cable-stayed girder bridge, Toyosato Ohhashi Bridge. (Fig. 1). Catastrophic motions and restricted motions were observed in this experiment. It was concluded that the formers appeared at so high wind velocities and the latters would not occur in a natural wind.
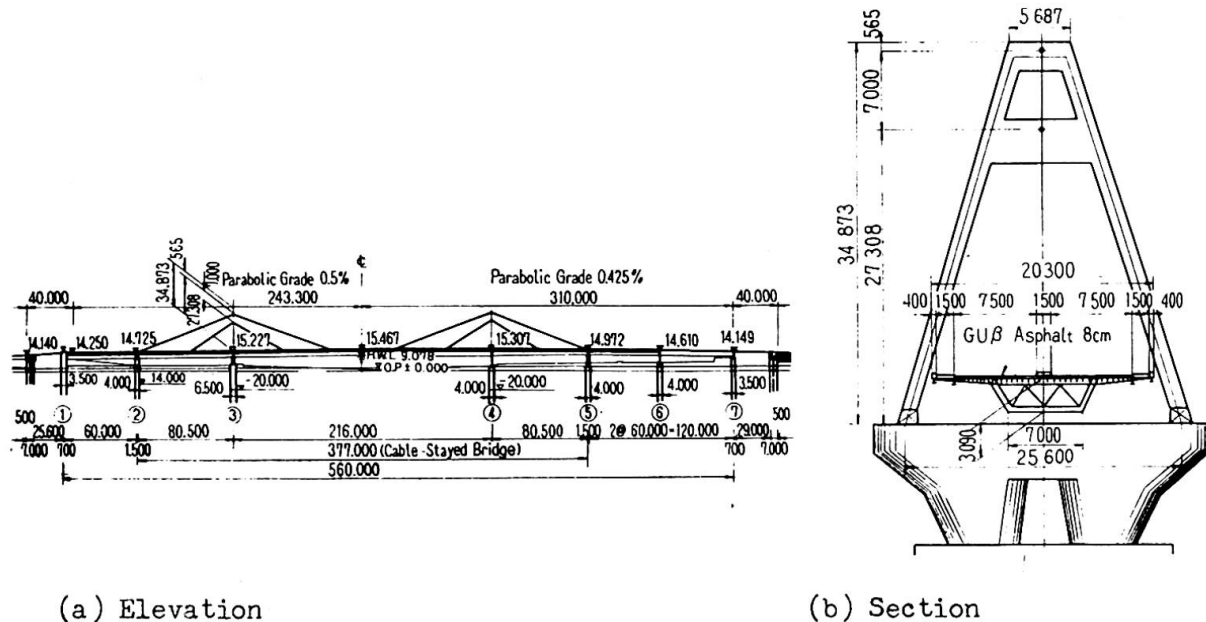
(a) Elevation   (b) Section
Fig. 1 General view of Toyosato Ohhashi Bridge

2. Wind Tunnel Experiment

2.1 Model

To perform a wind tunnel experiment, such a sectional model as indicated in Fig. 2 was selected. The model was reduced to 1/20 of the prototype. It consists of two kinds of parts, one is the moving model of 2.5 meters long (4 in Fig. 2). It has a supporting shaft along the center axis of the model (2 in Fig. 2). The other parts are end plates and dummy models of 0.1 meter long (1 and 3 respectively in Fig. 2). The existence of the end plates and dummy models will be useful for eliminating three-dimensional effects of a wind stream.

The model was manufactured minutely so that it might resemble the prototype in detail, and its weight and moment of inatia were 68.8kg and 65.8kg.cm. sec. respectively.

2.2 Test Procedures

The model was supported horizontally in the wind tunnel by using eight coil springs so as to move vertically in the plane of the tunnel cross section and

rotate about the supporting shaft and fixed by piano wires not to move windward. Natural frequency of the vertical vibration of the model was varied by changing a spring constant, and natural frequency of the rotational vibration was varied by changing a distance between the opposite springs. Structural damping of the model was varied by using magnet dumpers, changing an intencity of magnetic forces and a location of the dampers, and damping coefficients of the both of vertical and rotational vibration were controlled freely.

Accelerations and displacements of the vibrating model were measured by accelerometers of wire strain gauge type and linear transformers, respectively. Wind pressures were measured by an alcohl manometer.

Fig.2 Prototype and its wind tunnel model.

The tests were conducted at Reynold's numbers of $1.0 \times 10^5 / 2.0 \times 10^6$, which were considerably higher than at ordinary dynamic tests.

Static tests were conducted at constant Reynold's numbers of 6.7×10^5 and 1.0×10^6.

The typical examples of the dynamic tests are shown in Table 1.

2.3 Test Results
 (a) Static Tests
        The drag, lift and moment coefficients of air forces were calculated with measured data. There are no significant differences among each coefficient which is obtained at the different Reynold's number. These coefficients of the air forces are compared with the other types of models, namely a truss type and a wing type as indicated in Fig. 3.

 (b) Dynamic Tests
   i) Catastrophic Vibrations
        When an angle of attack for the model is zero degree, no catastrophic vibration can be observed in all the range of wind velocity, corresponding test numbers are A-1, 2, 3 in Table 1. When the angle of attack exists, catastrophic vibrations occur at relatively low wind velocities, corresponding test numbers are B-1, 2 and C-1, 2, 3, 4 in Table 1.

   ii) Restricted Vibrations

        When the model has a positive angle of attack, vibrations are observed at lower wind velocities than the velocity at which the catastrophic vibrations occur. These vibrations disappear when the wind velocity increases to some more high values. These phenomena are so cal-
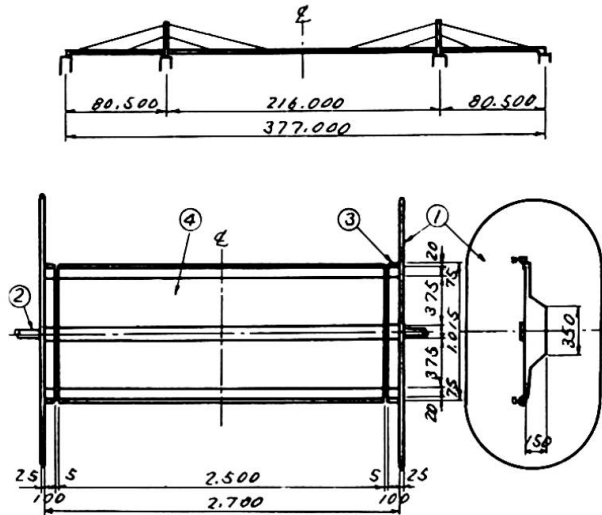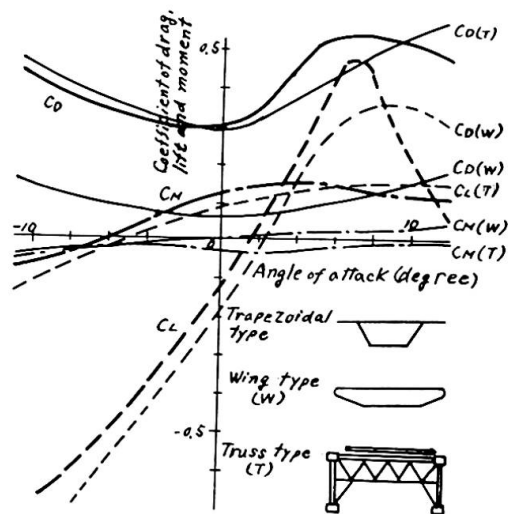

Fig.3 Coefficients of air forces compared with the other types of bridge sections.

led "restricted vibrations". Amplitude response curves of these phenomena are shown in Fig. 4 (a) and Fig. 4 (b).

Table 1. Summary of tests and results

Test number	α deg.	Nz c/s	$N\theta$ c/s	Vc m/s	Vz m/s	Tz sec	$V\theta$ m/s	$T\theta$ sec	Sz	$S\theta$
A – 1	0	4.28	5.25	119	–	–	–	–	–	–
A – 2	0	3.08	3.82	108	–	–	–	–	–	–
A – 3	0	3.11	3.27	200	–	–	–	–	–	–
B – 1	3	4.25	5.25	67	4.3	480	24	100	0.18	0.17
B – 2	3	5.00	5.22	52	4.1	480	17	105	0.18	0.17
C – 1	5	1.30	2.66	72	4.6	169	30	55	0.11	0.15
C – 2	5	3.07	3.83	59	4.0	250	31	–	0.11	0.14
C – 3	5	3.08	3.16	46	4.1	244	38	51	0.11	0.15
C – 4	5	3.10	2.57	86	4.8	185	31	–	0.11	0.19

Note: Nz, $N\theta$:   Frequency of model.
       Vc :   Critical Velocity for catastrophic vibration.
    Vz, $V\theta$:   Wind Velocity at which restricted vibration occur.
    Tz, $T\theta$:   Time during which amplitude of restricted vibration is growing.
    Sz, $S\theta$:   Strouhal number of model.
   Suffixes z and θ indicate vertical and rotational vibrations respectively.

It is well known that in case of the catastrophic vibration, the amplitudes grow rapidly in a short time to catastrophic magnitude from a rest position. On the contrary, the restricted vibrations observed in these tests were mild. It took a very long time to attain to stationary amplitudes.

The vertical or rotational vibration appeared independently with proper natural frequency. In some cases the both vibrations were observed at the same time, each frequency of the both vibrations were near its natural frequency and not combined together.

The damping coefficients of the model were changed and the corresponding response curves are shown in Fig.4 (a). The amplitudes decrease as the damping coefficients increase, but no strong relation between the amplitudes and the damping coefficient can be found in these tests.

The wind velocity at which the restricted vibration attains its maximum stationary amplitude is different in each test which has a different natural frequency and angle of attack. If the Strouhal numbers of the vibrating model are defined as follows: $S=Nh/V$, where N is vertical or rotational natural frequency
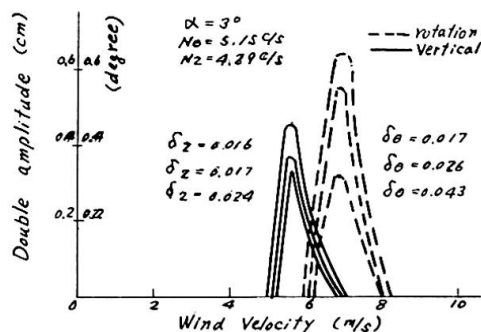

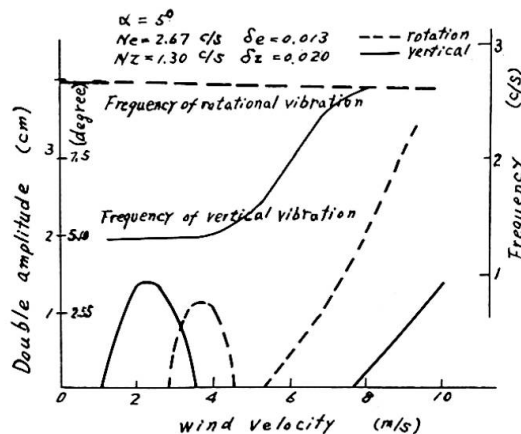Fig.4 (a) Amplitude response curves

Fig.4 (b) Amplitude response curves

of the model, h shows horizontal projection of a height of the model and V is wind
velocity at which the amplitude response attains the muximum value. In cases of
angle of attack α =5°, corresponding test numbers are C-1, 2, 3, in Table 1, the
Strouhal numbers are S $\doteq$ 0.17 for the rotational vibrations and S $\doteq$ 0.11 for the
vertical vibrations respectively. In cases of angle of attack α=3°, correspond-
ing test numbers are B-1, 2 in Table 1, the Strouhal numbers are S $\doteq$ 0.17 for
the both of the vertical and rotational vibrations.

K. Klöppel[4] and T. Yamaguchi[5] measured the Strouhal numbers of the models
whose cross sectional shapes were similar to the model handled in this paper.
They showed that the Strouhal numbers of the models were about S = 0.12. Their
models were simply designed and made of wooden plates, on the contrary the model
herein was closely resembled to a prototype having handrails, wheel guards, etc.
According to the cross sectional shape of the models, the frequencies of wake
voltices discharged from the models seem to be different from each other sensi-
tively. Those of the model herein were slightly higher than those of their
models, and the Strouhal numbers of the model herein were slightly enlarged.

3. Safety of Prototype

3.1 Critical Velocities for Catastrophic Vibrations

From the previous section the critical velocities at which the model caused
catastrophic vibration were obtained. The models were arranged to satisfy the
aerodynamic similarity, so the critical velocities of the model prototype could
be calculated from those of the model. The critical velocities of the prototype
are shown in Table 1. In cases of angle of attack α =0°, the critical veloci-
ties are very high. If a safety factor for the critical velocity of a catastro-
phic vibration is assumed as f = 1.2*), the allowable maximum wind velocity is
estimated from the critical velocity in Table 1 to be Va=Vc/f=Vc/1.2 . In cases
of angles of attack α=3° and α =5°, the critical velocities are relatively low
compared with a stormy wind velocity.

It will be necessary to examine if such critical velocities are dangerous
for the prototype or not. It is useful to apply the relation[6] between angle of
attack and velocity of a natural wind observed at the Severn Bridge in England
and the Akashi Narrows Bridge in Japan to examin the above question. (Fig.5).
According to the results of the above observations, the maximum wind velocity
drops as the angle of attack increases, the maximum wind velocities are found to
be 27 m/s and 10 m/s for the angles of attack of the wind α=3° and 5° respect-
ively, where the velocities are the average values during 30 seconds.

The prototype has been constructed at an open field, so that the above-
mentioned fact is applicable to this case. Namely, the prototype does not
cause a catastrophic vibration corresponding to the model which has a positive
angle of attack.

*) This value is specified at "Standard Specification for the design
   of the Honshu-Shikoku Renrakukyo (Long Span Suspension Bridge)
   against wind" 1967 (in Japanese).

3,2 Safety against restricted vibration

It has been studied that a restricted vibration appears at a very low wind
velocity, for example a vertical vibration occurs at the wind velocity V = 4m/s
if a natural wind flows having a positive angle of attack α=5°.

The amplitudes of restricted vibrations of the prototype were predicted
from the experimental data, using the theory by F. B. Farquarson[7]. The theory
is based on the following assumption that the aerodynamic damping in the wind
of a given velocity can be expressed by a power series equation of amplitude.
The amplitudes of the prototype predicted with the above theory are shown in

Table 2. In this calculation a vibration mode of the prototype was assumed to be of the first mode. In cases of vertical vibrations the amplitudes of the maximum fiber stresses are not so large, and in cases of rotational vibrations the amplitudes of the maximum shearing stresses are relatively large, however the corresponding wind velocities at which the amplitudes attain the maximum values are higher than those of the vertical vibrations.

Table 2. Maximum amplitudes and stresses of prototype due to restricted vibrations and corresponding wind velocities.

Test number	α deg	Vertical Vibration			Rotational Vibration		
		η max cm	σ max kg/cm^2	V m/s	θ max deg	τ max kg/cm^2	V m/s
B - 1	3	2.6	32	4.2	0.36	359	30
B - 2	3	5.1	62	4.6	0.28	244	30
C - 1	5	14.5	177	7.6	0.80	700	34
C - 2	5	13.9	170	8.3	-	-	40
C - 3	5	11.0	134	8.1	0.38	311	37
C - 4	5	11.6	141	8.5	0.52	455	30

As indicated above, the vertical restricted vibrations occur at very low wind velocities when the wind has an angle of attack. It is doubtful if the prototype actually vibrates in a natural wind as indicated in the next section, because the natural wind flows horisontally in average for time and space at an open field, and has an angle of attack fluctuating positively and negatively at random with a relatively high frequency. On the other hand, the restricted vibrations grow very slowly, it takes more than 100 seconds long to attain the maximum stationary amplitude from the rest position in the cases of the vertical vibrations.

4. Aerodynamic Behavior of Prototype in Turbulent Flow

To see whether the above assumption is true or not, the observations of natural wind have been made at the point where the prototype was constructed, and at the same time the behavior of the bridge due to wind has been observed.

No restricted vibration has been able to be observed so far. Vertical components of the wind were analyzed with the observed data. One of these is shown in Fig.6, in which the full lines show the theoretical values calculated from the power spectrum of vertical component of a wind proposed by H. A. Panofsky and R. A. McCormic[8]. This figure shows the maximum angle of attack of a wind as a function of time during which an angle of attack is averaged. In this case the mean wind velocity is about 10 m/s. The angle of attack of a wind decreases as the time increases.

It can be concluded that a wind does not continue to flow in the constant direction at negative or positive angle of attack for a long time,
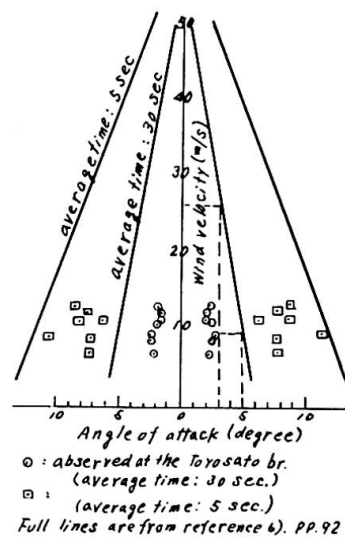

Fig.5. Wind velocity and angle of attack.

and such a wind can not develop a restricted vibration at all. That is to say, it is recognized that there is no natural wind which enables the prototype to cause the restricted vibration which was observed in the wind tunnel experiment.

5. Conclusions

The following results could be obtained from the wind tunnel experiment concerning to the cable-stayed girder bridge.

(1) When no angle of attack of a wind exists, this type of bridge is considerably stable in terms of an aerodynamic stability.

(2) When a positive angle of attack of stationary wind exists the model gives rise to the restricted vibrations at very low wind velocities.

Fig.6 Maximum angle of attack of natural wind.

(3) Both vertical and rotational amplitudes of the restricted vibrations of the prototype in the stationary wind were predicted. As a result, it was found that these amplitudes would not grow to a significant quantity.

(4) It takes more than 100 seconds for the vibration to attain a maximum stationary amplitude from its rest position in case of vertical vibration of the prototype.

(5) From the field measurements, it was found that a natural wind could not cause the restricted vibrations. Besides, no vibration of the prototype has been observed up to now.

Acknowledgment

References

(1) F. Bleich, Trans. ASCE, Vol. 114, No.2385 (1949).

(2) G. V. Perkinson and N. P. H. Brooks, Trans. ASME, Vol. 83 (1961) pp. 252--258.

(3) A. G. Davenport, Proc. ICE, Vol.19 (1961) pp.449--472.

(4) K. Klöppel and F. Thiele, Der Stahlbau, H-12 (1967) pp.353--365.

(5) T. Yamaguchi, et al, Mitsubishi Heavy Industries Tech. Review, Vol. 7, No.7 (1970), (in Japanese).

(6) K. Aoki, et al, "Supplementary Note to First Rep. of Tech. Investigation on the Honshu-Shikoku Br." JSCE, Tokyo, Japan (1964), (in Japanese) pp.91--92.

(7) F. B. Farquarson, et al, Bull. Univ. Washington, Eng. Station, No.116, Part V (1949--1954) pp.13--31.

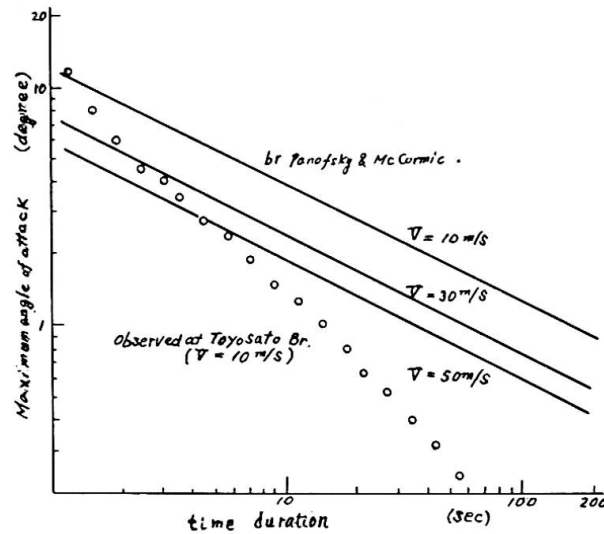(8) H. A. Panofsky and R. A. McCormic, Inst. Aero. Sci., Rep. Vol. 59, No.6 (1959).

Summary

Zu make clear the aerodynamic characteristics of a cable-stayed bridge
(Toyosato Ohhashi Bridge) with trapezoidal cross section, the wind tunnel
investigation has been carried out using two-dimensional model with linear
scale of 1:20 in comparatively high Reynold's number.

The investigation has shown that the aerodynamic instability will not be
induced in high wind which may be experienced at the site of actual bridge.

The small stationary amplitude vibrations, so-called restricted vibra-
tions, grew up slowly in smooth airflow inclined upwards 5 degrees to hori-
zontal. However, it is recognized from studying the three-dimensional effect
of actual bridge that the restricted vibration may not be considered to occur
in turbulent airflow such as natural wind which has been measured at the site.